9362–9378 *Nucleic Acids Research, 2015, Vol. 43, No. 19* *Published online 7 October 2015*
doi: 10.1093/nar/gkv988

MiRNA-891a-5p mediates HIV-1 Tat and KSHV Orf-K1 synergistic induction of angiogenesis by activating NF-κB signaling

Shuihong Yao[1,2,3,4,†], Minmin Hu[3,†], Tingting Hao[5,†], Wan Li[3,†], Xue Xue[3], Min Xue[3], Xiaofei Zhu[3], Feng Zhou[3], Di Qin[3], Qin Yan[3,*], Jianzhong Zhu[6], Shou-Jiang Gao[7] and Chun Lu[1,2,3,*]

[1]State Key Laboratory of Reproductive Medicine, Nanjing Medical University, Nanjing, P.R. China, [2]Key Laboratory of Pathogen Biology of Jiangsu Province, Nanjing Medical University, Nanjing, P.R. China, [3]Department of Microbiology, Nanjing Medical University, Nanjing 210029, P.R. China, [4]Medical School, Quzhou College of Technology, Quzhou 324000, P.R. China, [5]Department of Medical Laboratory, The Affiliated Hospital of Xuzhou Medical College, Xuzhou 221000, P.R. China, [6]Cancer Virology Program, University of Pittsburgh Cancer Institute, Pittsburgh, PA 15232, USA and [7]Department of Molecular Microbiology and Immunology, Keck School of Medicine, University of Southern California, Los Angeles, CA 90033, USA

Received May 11, 2015; Revised September 17, 2015; Accepted September 19, 2015

ABSTRACT

Co-infection with HIV-1 and Kaposi's sarcoma-associated herpesvirus (KSHV) is the cause of aggressive AIDS-related Kaposi's sarcoma (AIDS-KS) characterized by abnormal angiogenesis. The impact of HIV-1 and KSHV interaction on the pathogenesis and extensive angiogenesis of AIDS-KS remains unclear. Here, we explored the synergistic effect of HIV-1 Tat and KSHV oncogene Orf-K1 on angiogenesis. Our results showed that soluble Tat or ectopic expression of Tat enhanced K1-induced cell proliferation, microtubule formation and angiogenesis in chorioallantoic membrane and nude mice models. Mechanistic studies revealed that Tat promoted K1-induced angiogenesis by enhancing NF-κB signaling. Mechanistically, we showed that Tat synergized with K1 to induce the expression of miR-891a-5p, which directly targeted IκBα 3′ untranslated region, leading to NF-κB activation. Consequently, inhibition of miR-891a-5p increased IκBα level, prevented nuclear translocation of NF-κB p65 and ultimately suppressed the synergistic effect of Tat- and K1-induced angiogenesis. Our results illustrate that, by targeting IκBα to activate the NF-κB pathway, miR-891a-5p mediates Tat and K1 synergistic induction of angiogenesis. Therefore, the miR-891a-5p/NF-κB pathway is important in the pathogenesis of AIDS-KS, which could be an attractive therapeutic target for AIDS-KS.

INTRODUCTION

Kaposi's sarcoma-associated herpesvirus (KSHV) is a gamma herpesvirus, initially identified in a Kaposi's sarcoma (KS) lesion from an AIDS patient in 1994 (1). KSHV is also associated with several lymphoproliferative diseases, including primary effusion lymphoma (PEL) and multicentric Castleman's disease (MCD) (2). KS, which is a malignant vascular tumor characterized by abnormal blood vessel proliferation, includes four clinical subtypes: classic KS, AIDS-related KS (AIDS-KS), Africa endemic KS, and immunosuppressive/transplantation KS (3). KS lesions primarily consist of proliferative spindle cells expressing markers of vascular endothelial, lymphatic endothelial and precursor cells with vast infiltration of inflammatory cells (4). Like other herpes viruses, KSHV life cycle consists of latent and lytic replication stages. During the latency, KSHV only expresses a few latent genes, which is essential for maintaining latent infection and escaping immune surveillance. In KS tumors, the majority of the tumor cells are latently infected by KSHV. However, a small number of KSHV-infected cells also undergo lytic replication. Several lytic genes, including Orf-K1, vIRF1 (Orf-K9), vGPCR (Orf74) and vIL-6 (Orf-K2) are known to contribute to KSHV-induced pathogenesis (3,5). These genes promote tumor growth by regulating cell cycle and apoptosis, and by inducing pro-inflammatory and pro-angiogenic factors including

*To whom correspondence should be addressed. Tel: +86 25 86862910; Email: clu@njmu.edu.cn
Correspondence may also be addressed to Qin Yan. Tel: +86 25 86862910; Email: yanqin@njmu.edu.cn
†These authors contributed equally to this work.

vascular endothelial growth factor (VEGF) and basic fibroblast growth factor (bFGF) (3,6–10).

KSHV encoded Orf-K1 is a viral oncogene. The Orf-K1 is composed of 289 amino acids (aa), with a molecular weight of ∼46 kDa (11,12). The Orf-K1 protein can transform mouse fibroblasts and primary human umbilical vein endothelial cells (HUVEC), inhibit apoptosis, and promote cell proliferation, tumor angiogenesis and tumor formation (10,13–15). It activates the PI3K/Akt/mTOR, phospholipase PLC-γ, nuclear factor (NF)-κB (NF-κB), and AP-1 signaling pathways, leading to the expression of various growth factors and inflammatory cytokines, such as VEGF, bFGF, tumor necrosis factor (TNF)-α, IL-6, and IL-8 (16). Further, Orf-K1 induces the expression of matrix metalloproteinase (MMP)-9 in endothelial cells, which promotes tumor cell metastasis (13). By activating Rac1, VE-cadherin, and β-catenin, Orf-K1 also increases the vascular permeability of endothelial cells (17). In addition, Orf-K1 activates the VEGF/VEGFR2 pathway to stimulate endothelial cells through autocrine or paracrine mechanisms (5,10). Thus, Orf-K1 is likely play an important role in the pathogenesis of KS.

While KSHV infection is necessary, other co-factors can also promote the development of KS. One such co-factor is HIV-1 coinfection (18). Although HIV-1 and KSHV do not infect the same cell type (19), HIV-1 promotes KS formation by expressing a number of secretory proteins (20,21). For instance, HIV-1 transactivator of transcription (Tat) and negative factor (Nef) are released into the bloodstream from HIV infected cells, which could regulate the development of AIDS-KS (22–24). HIV-1 Tat is a multifunctional protein of 86–101 aa. Tat activates HIV-1 gene expression by binding to the transactivation response element in the long terminal repeat of HIV-1 (25). Tat is released into the tissues and blood of HIV-infected patients through a unique mechanism, which is independent of the endoplasmic reticulum and Golgi apparatus. Tat acts on the surface receptors of cells, or directly enters the cells and traffic to the cytoplasm and nucleus to regulate cellular genes in an autocrine and paracrine mechanism (9,26–29). Importantly, Tat is readily detected in spindle cells of AIDS-KS lesions and promotes the growth of KS-derived endothelial cells, thus might play a crucial role in the initiation and progression of KS in AIDS patients (30–32). Studies from our group and others have suggested that Tat activates KSHV lytic replication through the JAK/STAT pathway (23,33), and potentiates effects of KSHV oncogenic proteins, including vGPCR, Kaposin A and vIL-6, on cell proliferation and tumorigenesis in nude mice (22,34,35). In addition, Tat promotes KSHV-enhanced tumorigenesis by synergistically inducing the secretion of TNF-α, bFGF and other cytokines, (9,36).

It is well known that tumorigenesis and angiogenesis are inseparable in cancer, and KS tumor has a prominent abnormal vascular proliferation. In this study, we investigated the synergistic effect of Tat and K1 on angiogenesis. We found that Tat promoted the K1-induced angiogenesis through activation of the NF-κB signaling. This is due to the suppression of IκBα through synergistic induction of cellular miR-891a-5p by Tat and K1. Our results contribute to the understanding of the molecular mechanisms of AIDS-KS pathogenesis.

MATERIALS AND METHODS

Cells, plasmids, transfection and reagents

HEK293T and EA.hy926 cell lines were purchased from ATCC (Manassas, VA, USA), and cultured in Dulbecco's Modified Eagle's Medium (DMEM) containing 10% inactivated fetal bovine serum (FBS), 2 mmol/l L-glutamine (100 U/ml), penicillin and streptomycin (100 g/ml), in a 5% CO_2 incubator at 37°C. EA.hy926 is an immortalized cell line obtained from fusion of primary human umbilical vein cells (HUVEC) and the A549 human lung adenocarcinoma cell line, which has the characteristics of vascular endothelial cells (37). Primary HUVEC were cultured in EBM-2 culture medium (LONZA, Allendale, NJ, USA) (38,39), and cells of third to sixth generation were used in this study. IκB dominant negative plasmid (IκB-DN) with Flag tag was cloned into lentiviral pCDH vectors by PCR. NF-κB reporter plasmid containing three repetitive sequence (tandem repeats) binding sites was prepared as described previously (40). The IκBα 3′UTR was cloned into the downstream of luciferase reporter gene of pGL-3 Control vector to create wild type pGL-3-IκBα-3′UTR (WT IκBα) plasmid as previously described (41). Bioinformatics analysis software tools, including PITA, RNAhybrid and RNA22, were used to analyze and predict the binding sites between miR-891a-5p and 3′UTR of IκBα. The construction of the pGL-3-IκBα-3′UTR mutant plasmid (Mut IκBα) with mutated binding sites was made by site-directed mutagenesis. Recombinant HIV-1 Tat protein (soluble Tat) with His tag was purchased from Abcam (Cambridge, MA, USA). NF-κB inhibitor Bay11–7082 was purchased from Sigma (St Louis, MO, USA). The membrane matrix (BD Matrigel Basement Membrane Matrix) was obtained from BD Biosciences (Bedford, MA, USA). The transfection reagent for HUVEC was Effectene (Qiagen, Valencia, CA, USA), and other types of transfection were performed using Lipofectamine 2000 (Invitrogen, Carlsbad, CA, USA).

Lentivirus preparation and transfection

Lentivirus was prepared as previously described (22,38). In this study, HUVEC were treated with soluble Tat protein, while EA.hy926 cells were transduced with lentivirus expressing Tat (Tat) as previously described (22). Specifically, HUVEC were first transduced with lentivirus expressing K1 (K1) and then treated with soluble Tat protein, while EA.hy926 cells were transduced with lentivirus expressing K1 and Tat.

Cell Counting Kit (CCK-8) for cell proliferation assay

Cell Count Kit-8 was purchased from Dojindo Molecular Technologies (Tokyo, Japan) and used to examine cell proliferation according to the manufacturer's instructions.

Plate colony formation assay

Cells were digested and counted, the 100 μl cell suspension (containing 100 cells) seeded into 24-well culture plates and

the culture medium was made up to 1 ml, and then cultured in a 5% CO_2 incubator at 37°C. The culture plate was collected 14 days later, and the cell colony numbers were directly counted after crystal violet staining.

Microtubule formation assay

Microtubule formation assay was performed as previously described (21,22,38). Relative angiogenesis was evaluated according to microtubule formation index calculated as previously described (42).

Chorioallantoic membrane (CAM) assay

CAM assay was performed as previously described (22). Briefly, 8-day-old embryos from SPF grade White Leghorn chicken were selected. Cells transduced with K1, Tat, or both were mixed with Matrigel, before being vertically inoculated onto the CAM through the false gas chamber hole. After incubation in 80–90% relative humidity at 37°C for 4 days, the CAM was harvested and examined under stereomicroscopy.

Matrigel plug assay for angiogenesis in nude mice

Matrigel plug assay was performed as previously described (38). Briefly, EA.hy926 cells transduced with K1, Tat, or both were mixed with Matrigel at a ratio of 1:2, and inoculated on the back flank of 3–4-week-old male BALB/c nude mice (Shanghai Silaike Experimental Animal Center, Shanghai, China). The animals were sacrificed 10 days later, and the inoculum (Matrigel plug) was peeled off and photographed under stereomicroscopy. Small pieces of tissue were cut out and weighed, which were processed using the Drabkin's reagent kit (Sigma–Aldrich, St Louis, MO, USA) with spectrophotometric analysis at 540 nm, followed by calculation of hemoglobin content based on the standard curve obtained.

Tumorigenicity assay in nude mice

Tumorigenicity assay in nude mice was performed as previously described (21,35). Suspensions of EA.hy926 cells expressing target protein at concentration of $1 \times 10^7/100$ μl (1×10^7 cells per animal) were subcutaneously (sc) injected into the left flanks of nude mice. The occurrence and size of the tumor was observed and recorded daily for 7 days. The long diameter and perpendicular short diameter of the tumor were measured by vernier caliper, with the volume calculated according to the formula: volume = long diameter × short diameter × short diameter/2. The animals were sacrificed when the tumor reached a certain volume, with the tumor tissue peeled off immediately, photographed and weighed, which was immediately frozen, fixed in formalin, and embedded in paraffin for immunohistochemical staining, or homogenated with tissue protein extracted for Western blotting detection.

miRNA mimics, inhibitors and sponge

The sequence of commercially available miR-891a-5p mimic was 5′-UGCAACGAACCUGAGCCACUGA-3′; the sequence of miR-891a-5p mut mimic was 5′-UGGUUC GAACCUGAGCCACUGA3′; and the negative control sequence was 5′-UUCUCCGAACGUGUCACGUTT-3′. miRNA mimics, mut miRNA mimic and miRNA inhibitors were purchased from Shanghai Zimmer Pharmaceutical Company (Shanghai, China). A miRNA sponge for miR-891a-5p was used to inhibit its function. It contains multiple, tandem complementary binding sites for miR-891a-5p. When transduced into the target cells, the miRNA sponge acts on the target miRNA miR-891a-5p by a base-pairing mechanism and depresses the miRNA. This technology achieves the same results as the miRNA inhibitors (43). As previously described (38), miR-891a-5p sponge was annealed and cloned into pCDH-CMV-MCS-EF1-copGFP vector (System Biosciences, Mountain View, CA, USA) through the upstream and downstream primers (upstream sequence: 5′-GAATTCTCAGTGGC TCCCATCGTTGCACGATTCAGTGGCTCCCATC GTTGCAACCGGTTCAGTGGCTCCCATCGTTGC ATCACTCAGTGGCTCCCATCGTTGCATCAGTG GCTCCCATCGTTGCACGATTCAGTGGCTCCCA TCGTTGCAGGATCC-3′, downstream sequence: 5′-GGATCCTGCAACGATGGGAGCCACTGAATCGT GCAACGATGGGAGCCACTGATGCAACGATGGG AGCCACTGAGTGATGCAACGATGGGAGCCACT GAACCGGTTGCAACGATGGGAGCCACTGAATC GTGCAACGATGGGAGCCACTGAGAATTC-3′). The empty plasmid pCDH-CMV-MCS-EF1-copGFP (pCDH) was used as the control. The lentiviral miR-891a-5p sponge and its control pCDH were packaged as mentioned above. In this study, to evaluate the short-term effect of inhibiting miR-891a-5p, we used miR-891a-5p inhibitor in microtubule formation and CAM assays, but for the long-term effect of inhibiting miR-891a-5p, we used a miR-891a-5p sponge in plate colony formation and Matrigel plug assays.

miRNA microarray analysis

miRNA microarray analysis was performed as previously described (38,44).

Luciferase reporter assay

Luciferase reporter assay was performed as previously described (38,45). The miRNA mimics, IκBα 3′UTR luciferase reporter plasmid and Renilla vector pRL-TK were co-transfected into HEK293T cells, with the luciferase activity determined as described above.

Antibodies, Western blotting and other reagents

Anti-phospho-NF-κB p65 (Ser536) rabbit polyclonal antibody (pAb) was purchased from Santa Cruz Biotechnology (Santa Cruz, CA, USA). Anti-NF-κB p65 rabbit pAb was obtained from Abcam (Cambridge, MA, USA). IκBα monoclonal antibody (mAb), His mAb, and Flag mAb were purchased from Cell Signaling Technology (Danvers, MA, USA). GAPDH mAb, tubulin mAb, VEGF mAb, smooth muscle actin (SMA) pAb, horseradish-peroxidase-labeled goat anti-mouse and goat anti-rabbit IgG were purchased from Santa Cruz Biotechnology (Santa Cruz). Western blotting was carried out as described previously (46,47).

IMD 0354, an IKKβ inhibitor, was obtained from Selleck Chemicals (Shanghai, China).

Confocal microscopy

Cells were seeded in glass-bottom Petri dishes, with soluble Tat protein added for 24 h, as previously described (21). Mouse anti-NF-κB p65 mAb (Cell Signaling Technology) and Alexa-Fluro-647-labeled goat anti-mouse secondary antibody (Invitrogen) were added, followed by nuclear staining of the cells by 4′,6-amidine-2-phenylindole (DAPI). The stained cells were examined and photographed using a Zeiss Axiovert 200M laser scanning confocal microscope (Carl Zeiss, Freistaat Thuringen, Germany).

NF-κB/p65 DNA-binding activity assay

Nuclear protein was extracted using the Active Motif nuclear extraction kit (Carlsbad, CA, USA), followed by determination of the NF-κB p65 DNA binding activity (TransFactor NF-κB p65 ELISA Kit; Clontech Laboratories, Mountain View, CA, USA). In order to ensure specificity, a competitive oligonucleotide was added to the nuclear protein as a positive control. The OD_{630} was measured with a microplate reader as previously described (48,49).

Hematoxylin and eosin (H&E) and immunohistochemical staining

The CAM and tumor tissues of nude mice were made into frozen paraffin sections immediately after harvest. Then they underwent H&E staining for pathologic observation and immunohistochemical staining for the detection of SMA, VEGF and NF-κB p65 expression as previously described (35).

Real-time quantitative reverse transcription-PCR (RT-qPCR)

Total RNA was isolated from cells by Trizol reagent (Invitrogen). RT-qPCR was performed using SYBR *Premix Ex Taq*™ Kit (TaKaRa Biotechnology Co. Ltd, Dalian, China) according to the manufacturer's instructions. The quantification of miRNAs was performed by stem-loop RT-qPCR as previously described (41,45). The Bulge-Loop miR-891a-5p primers were synthesized by Ribo Biotechnology (Guangzhou, China). The sequences of specific primers of RT-qPCR for IκBα were: upstream sequence, 5′-AATT GCTGAGGCACTTCTGG-3′; downstream sequence, 5′-TAGCCTTCAGGATGGAGTGG-3′.

Statistical analysis

SPSS version 18.0 was used for the statistical analysis of experimental data, with data presented as mean ± standard error of mean (SEM). Differences with $P < 0.05$ were considered statistically significant. All the experiments were repeated three times, unless otherwise stated.

RESULTS

HIV-1 Tat protein synergizes with KSHV Orf-K1 to induce cell proliferation and microtubule formation *in vitro* by activating the NF-κB pathway

We conducted cell proliferation, colony formation and microtubule formation assays to determine whether there were synergistic effects between HIV-1 Tat and KSHV Orf-K1. To examine the effect of Orf-K1, we transduced Orf-K1 in either HUVEC or EA.hy926 cells. To examine the effect of Tat, we either directly incubated soluble Tat with HUVEC or transduced Tat in EA.hy926 cells. Ectopic expression of K1 alone increased the proliferation rates of HUVEC and EA.hy926 cells (Figure 1A). Tat also increased cell proliferation in HUVEC and EA.hy926 cells. Interestingly, Tat and K1 synergized with each other and further increased the cell proliferation rate (Figure 1A). Plate colony formation assay can measure the proliferative activity of single and multiple cells (50). In this assay, Tat or K1 alone increased colony formation of EA.hy926 cells and synergized with each other to further increase cell proliferation (Figure 1B). Further, in an *in vitro* microtubule formation assay, compared to control cells (Mock + PBS), K1 or Tat increased tube formation by 2.33- and 2.70-fold in HUVEC, respectively, while Tat synergized with K1 to further increase tube formation by 6.24-fold (Figure 1C and D). Similar results were observed in EA.hy926 cells (Figure 1C and D).

To identify the mechanism mediated K1 and Tat promotion of angiogenesis, we examined the expression of key molecules associated with the angiogenic pathways. In HUVEC and EA.hy926 cells, Tat or K1 alone induced the degradation of intracellular IκBα, and Tat and K1 further manifested synergistic effect to degrade IκBα (Figure 2A). Importantly, the expression level of VEGF was negatively correlated with that of IκBα (Figure 2A), suggesting that Tat and K1 might induce the expression of VEGF by activating the NF-κB pathway. Indeed, Tat or K1 increased the level of phosphorylated p65 (Figure 2A), p65 nuclear translocation (Figure 2B), the binding of p65 to the NF-κB consensus site (Figure 2C), and the activity of a NF-κB reporter (Figure 2D). Tat and K1 further synergized with each other to activate the NF-κB pathway (Figure 2A–D).

Tat synergistically promotes K1 in inducing angiogenesis in CAM and nude mice models

The above results showed that Tat synergized with K1 to induce microtubule formation in endothelial cells *in vitro*. We further confirmed these results in an *in vivo* HUVEC-induced CAM angiogenesis model. Tat, K1 or both increased the angiogenesis index by 2.22-, 2.17- and 4.89-fold, respectively (Figure 3A and B). Similar results were observed in the CAM model induced by EA.hy926 cells (Figure 3B).

H&E staining of the tumor tissues showed induction of tumor angiogenesis and red cell infiltration in the K1 or Tat group with the highest aggregation of tumor cells and angiogenesis observed in the K1 plus Tat group (Figure 3C top). Immunohistochemistry showed the expression of SMA, a marker of the vascular and lymphatic endothelial cells, and VEGF, a pro-angiogenic factor. The levels of

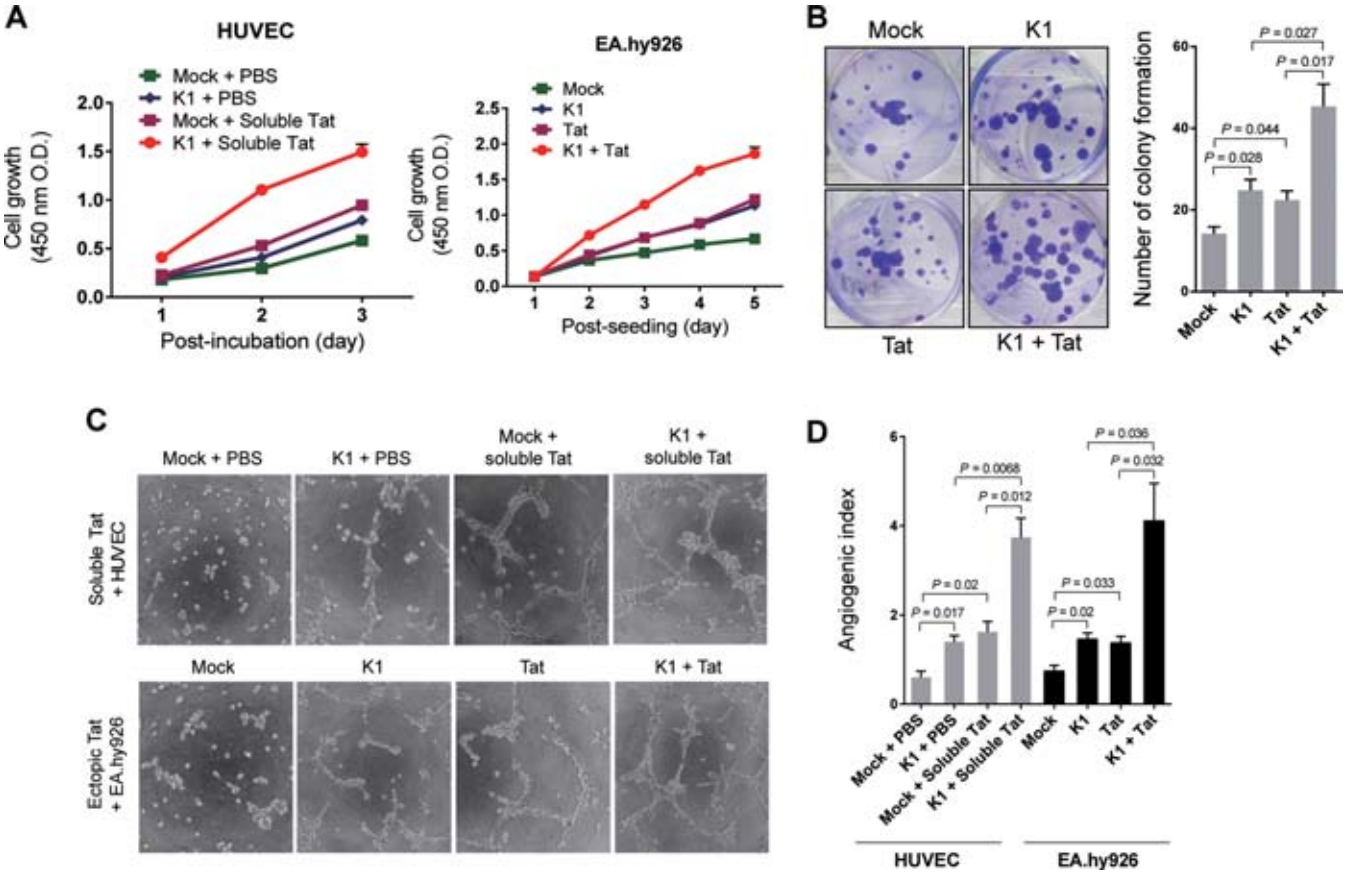

Figure 1. Tat synergistically facilitates K1 in promoting endothelial cell proliferation and microtubule formation. (**A**) Endothelial cell proliferation. Primary HUVEC transduced with lentiviral K1 or the control empty vector Mock were incubated with soluble Tat (200 ng/mL) and further examined with CCK-8 assay on days 1, 2 and 3 (left). EA.hy926 cells transduced with lentiviral K1, Tat, or both (K1 + Tat), as well as the control empty vector Mock were seeded and examined for cell proliferation with CCK-8 test on days 1, 2, 3, 4 and 5 (right). Data represent mean ± SEM determined from three independent experiments ($n = 3$), each experiment containing six technical replicates. (**B**) Plate colony formation assay. EA.hy926 cells treated as described in (A) were digested into single cells, seeded, and cultured for 14 days, followed by crystal violet staining with the size and number of formed colonies measured (left). The histogram demonstrates the quantification of colony formation (right). Data represent mean ± SEM determined from three independent experiments ($n = 3$), each experiment containing five technical replicates. (**C**) Microtubule formation assay. HUVEC and EA.hy926 cells treated as described in (A) were seeded onto the culture plate with Matrigel and photographed under microscopy (×100) 16 h later. (**D**) Quantification of the results in (C). Data represent mean ± SEM determined from three independent experiments ($n = 3$), each experiment containing six technical replicates.

both SMA and VEGF were significantly increased in tumors induced by K1, Tat, or both (middle and bottom panels in Figure 3C and D). Consistent with the *in vitro* results, Tat markedly promoted the degradation of IκBα in the K1-induced CAM tumor tissues. Accordingly, the VEGF expression was much higher in the presence of both K1 and Tat, which was consistent with that of immunohistochemical staining (Figure 3E).

To further confirm these observations, we performed Matrigel plug assay. EA.hy926 cells transduced with K1, Tat or both were mixed with Matrigel and subcutaneously inoculated into the back of the nude mice. In K1 plus Tat-induced tumor tissues, the number of blood vessels and red blood cell infiltration were notably increased (Figure 3F). The hemoglobin content of the tumor plug was increased by 1.61-, 1.43- and 3.95-fold in the K1, Tat, and both groups, respectively, compared with that of the Mock group (Figure 3G). These data suggest that Tat synergized with K1 in inducing angiogenesis *in vivo*.

NF-κB signaling mediates Tat and K1 synergistic induction in angiogenesis and tumor formation

To examine the role of NF-κB signaling in mediating the synergistic effect of Tat- and K1-induced angiogenesis, HUVEC with K1, soluble Tat protein or both were transduced with lentiviral IκB-DN and subsequently implanted onto CAMs. IκB-DN completely inhibited angiogenesis induced by K1, soluble Tat or both in the HUVEC-induced angiogenesis CAM model (Figure 4A). IκB-DN also drastically inhibited nuclear p65 binding to the NF-κB consensus site induced by K1, soluble Tat or both in cells isolated from the HUVEC-induced angiogenesis CAM model (Figure 4B). Bay11–7082 suppresses the NF-κB pathway by preventing the degradation of IκB through inhibition of its phosphorylation (51). Thus, we performed the angiogenesis assay with EA.hy926 cells transduced by K1, Tat or both in the presence of Bay11–7082. In the CAM model, the angiogenesis index was significantly decreased in the three groups of cells treated with Bay11–7082 compared with the control group (DMSO) (Figure 4C). As expected, treatment with Bay11–

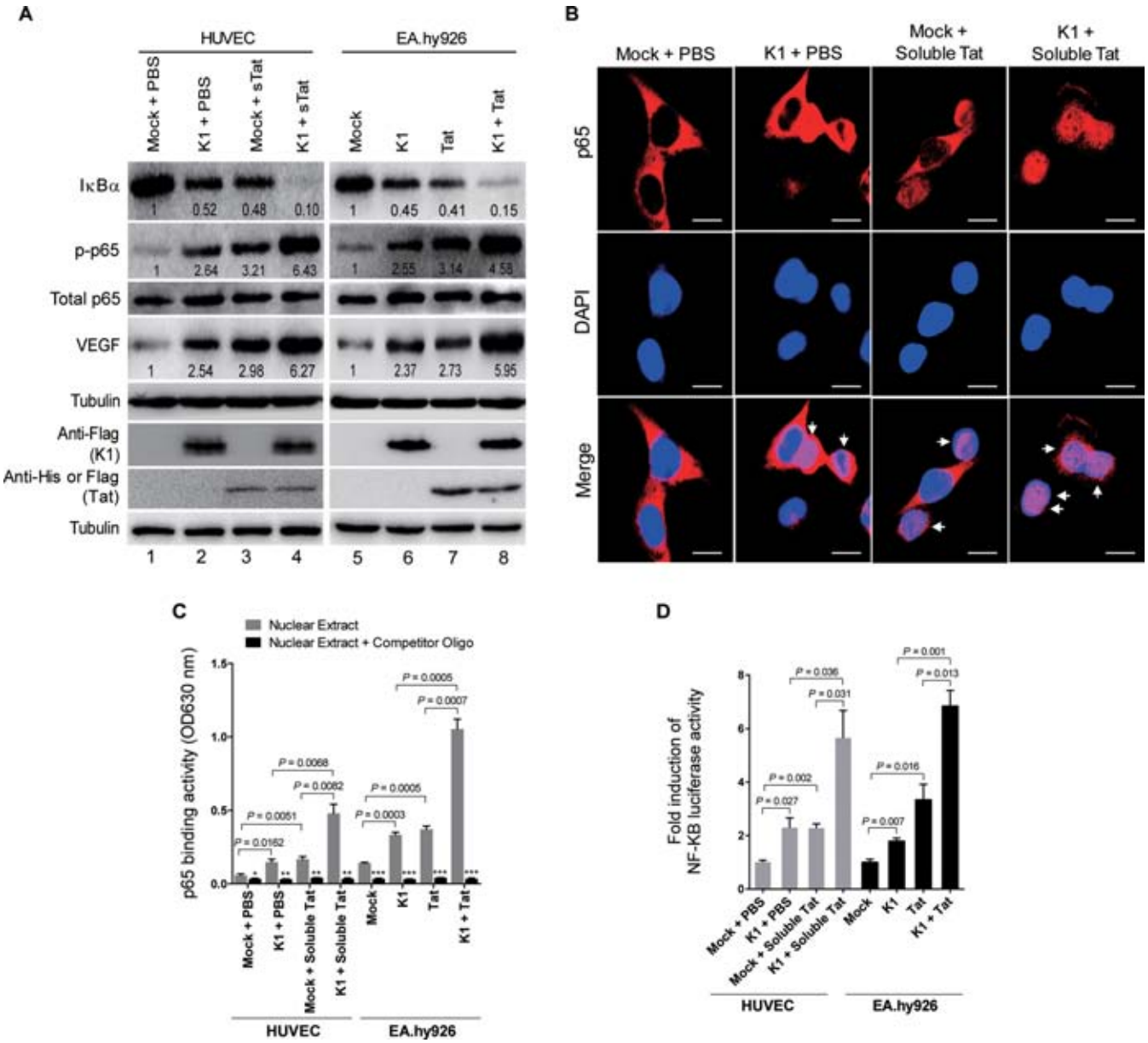

Figure 2. Tat synergistically promotes K1 in activation of NF-κB signaling. (**A**) Western blotting analysis of IκBα, phosphorylated p65, total p65 and VEGF in HUVEC transduced with K1, incubated with soluble Tat protein or both for 72 h (left panel), and EA.hy926 cells transduced with K1, Tat or both for 72 h (right panel), respectively. Expressions of K1 and ectopic Tat in cells were detected using anti-Flag-Tag antibody, while soluble Tat was examined using anti-His-Tag antibody. Numbers labeled under the bands were the relative intensities of the bands after calibrating for loading using house-keeping protein. The relative values of proteins in Mock + PBS group or Mock group was considered as '1'; same for all of the following western blotting figures. (**B**) Expression and nuclear translocation of p65 observed by confocal microscopy. HUVEC were treated as described in (A) for 24 h. Red represents expression and distribution of p65, and blue nuclear staining by DAPI. (**C**) NF-κB p65–DNA binding activity assay. Nuclear proteins were extracted from cells treated as described in (A), followed by determination of ELISA. Competitive oligonucleotide was used as a positive control and data represent mean ± SEM determined from three independent experiments ($n = 3$), each experiment containing three technical replicates. Compared with competitive oligonucleotide: $^{*}P < 0.05$, $^{**}P < 0.01$, and $^{***}P < 0.001$. (**D**) Detection of NF-κB activity by luciferase assay. Data represent mean ± SEM determined from three independent experiments ($n = 3$), each experiment containing four technical replicates.

7082 down-regulated DNA binding activity of p65 in cells of all groups (Figure 4D). In the Matrigel plug test, IκB-DN drastically suppressed the number of blood vessels and red blood cell infiltration, and significantly reduced hemoglobin content of tumors induced by Tat, K1 or both (Figure 4E and F). Furthermore, IκB-DN inhibited IκBα degradation in tumors induced by Tat, K1 or both (Figure 4G). To further confirm the specificity of NF-κB signaling in mediating the synergistic effect of Tat- and K1-induced angiogenesis, we used IMD 0354, an IKKβ inhibitor, in the angiogenesis assay. As expected, IMD 0354 not only inhibited the activity of a NF-κB reporter, but also reduced hemoglobin content of tumors induced by Tat, K1 or both in EA.hy926 cells (Supplementary Figure S1A and S1B). Consistently, IMD

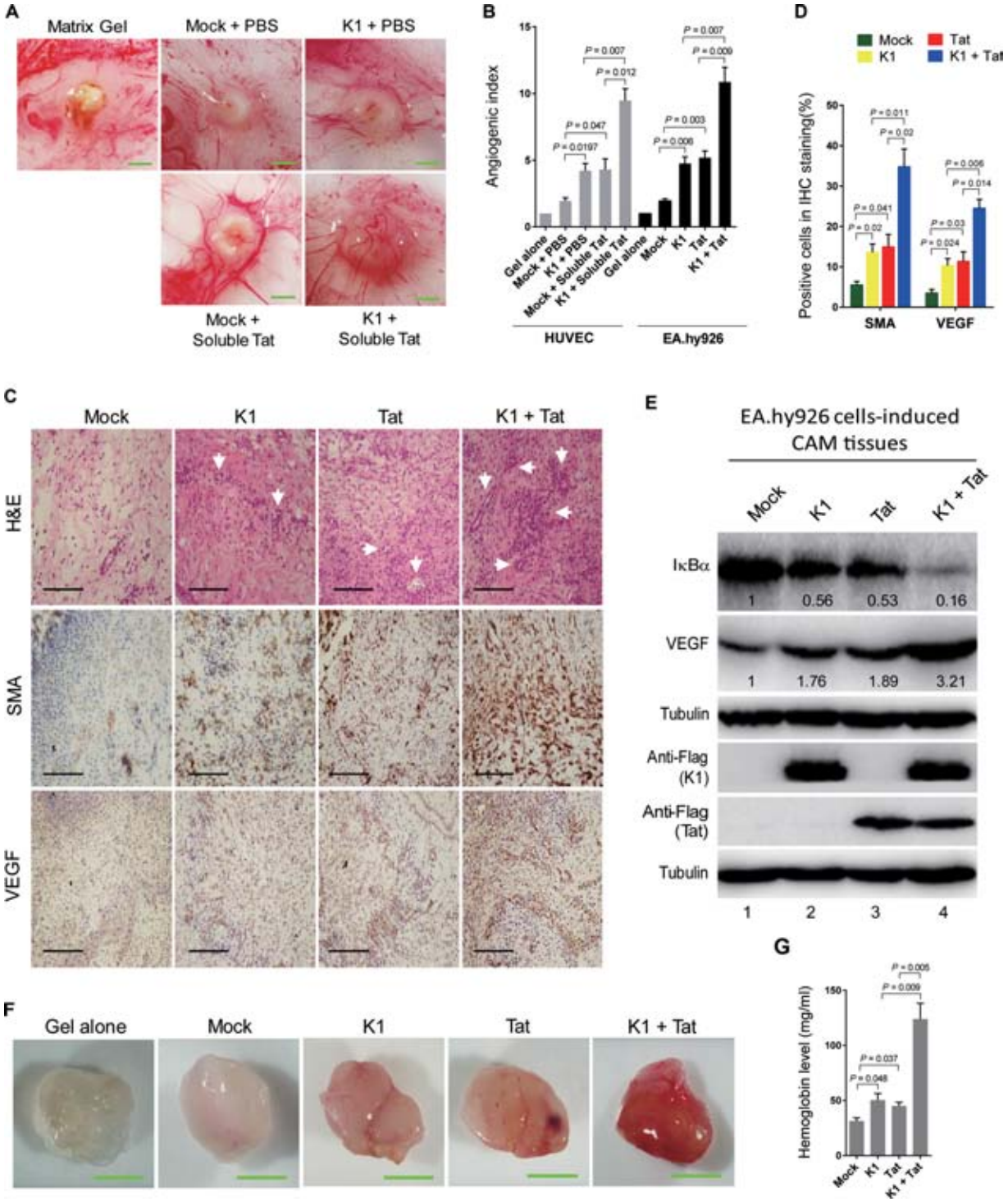

Figure 3. Tat synergized with K1 to promote angiogenesis in CAM and nude mice Matrigel plug angiogenesis models. (**A**) Tat promoted K1-induced angiogenesis of endothelial cells in the CAM model. HUVEC transduced with K1, incubated with soluble Tat protein or both for 72 h were mixed with Matrigel and implanted onto CAM. Representative photographs of angiogenesis on the CAM are shown under stereomicroscopy. (**B**) Quantification of results in (A). The number of blood vessels was normalized to that of Matrigel alone. Data represent mean ± SEM from three independent experiments ($n = 3$), each experiment containing six technical replicates. (**C**) Hematoxylin and eosin staining analysis of histologic features (top; ×200) and immunohistochemical staining analysis of the expression of SMA and VEGF (middle and bottom;×200) in tumor tissues from the CAMs induced by EA.hy926 cells transduced with K1, Tat or both. White arrows point to the formation of new blood vessels and hemorrhagic region. (**D**) Quantification of the results in (C). (**E**). Western blotting analysis of IκBα and VEGF in CAM tissues treated as in (C). (**F**) Tat promoted K1-induced angiogenesis in nude mice. EA.hy926 cells transduced by K1, Tat or both were examined for their proangiogenic effects in Matrigel plug assay in nude mice as described in the "Materials and Methods" section. Representative photographs of angiogenesis in the nude mice are shown. (**G**) The hemoglobin level of the Matrigel plugs treated as in (F) was determined with hemoglobin content calculated based on the standard curve. Data represent mean ± SEM determined from three independent experiments ($n = 3$), each experiment containing six technical replicates.

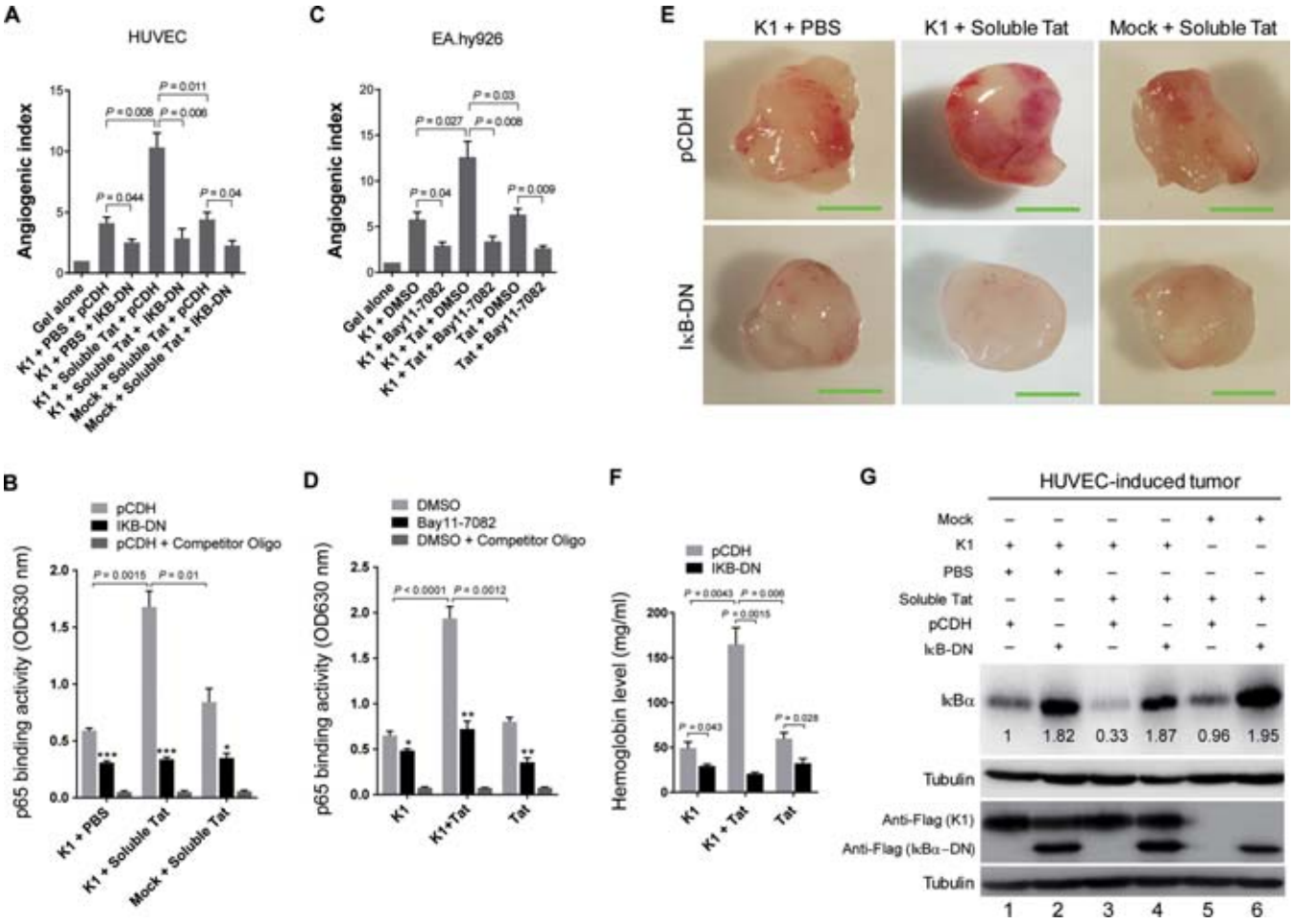

Figure 4. NF-κB pathway mediates synergistic effect of Tat in K1-induced angiogenesis. (**A**) Transduction of lentiviral IκB-DN inhibited angiogenesis in the CAM model. Lentiviral K1-transduced HUVEC were incubated with soluble Tat and subsequently transduced with lentiviral IκB-DN and its control vector pCDH. Cells were mixed with Matrigel and implanted onto CAM. The number of blood vessels was normalized to that of Matrigel alone. Data represent mean ± SEM from three independent experiments ($n = 3$), each experiment containing six technical replicates. (**B**) NF-κB p65–DNA binding activity assay. Nuclear proteins were extracted from CAM tissues treated as described in (A), followed by determination of ELISA. Competitive oligonucleotide was used as a positive control and data represent mean ± SEM determined from three independent experiments ($n = 3$), each experiment containing three technical replicates. Compared with competitive oligonucleotide: $^{*}P < 0.05$ and $^{***}P < 0.001$. (**C**) Bay11–7082 inhibited angiogenesis in the CAM model. EA.hy926 cells expressing K1, Tat and both were pretreated with Bay11–7082 or DMSO (control) for 3 h, and mixed with pre-cooled Matrigel and then inoculated into the CAM. The number of blood vessels was normalized to that of Matrigel alone. Data represent mean ± SEM from three independent experiments ($n = 3$), each experiment containing 6 technical replicates. (**D**) NF-κB p65–DNA binding activity assay. Nuclear proteins were extracted from CAM tissues treated as described in (C), followed by determination of ELISA. Data represent mean ± SEM determined from three independent experiments ($n = 3$), each experiment containing three technical replicates. Compared with competitive oligonucleotide: $^{*}P < 0.05$ and $^{**}P < 0.01$. (**E**) Transduction of lentiviral IκB-DN inhibited angiogenesis in nude mice model. Lentiviral K1-transduced HUVEC were incubated with soluble Tat and subsequently transduced with lentiviral IκB-DN and its control vector pCDH. Cells were examined for their proangiogenic effects in Matrigel plug assay in nude mice. Representative photographs of angiogenesis in the nude ice are shown. (**F**) The hemoglobin level of the Matrigel plugs treated as in (E) was determined with hemoglobin content calculated based on the standard curve. Data represent mean ± SEM determined from three independent experiments ($n = 3$), each experiment containing six technical replicates. (**G**) Western blotting analysis of IκBα in plug tissues from nude mice treated as in (E).

0354 suppressed the IκBα degradation in tumors induced by Tat, K1 or both (Supplementary Figure S1C).

It is well known that angiogenesis promotes tumor development. Since Tat and K1 could synergize with each other in inducing angiogenesis (Figure 3), we investigated whether Tat might affect K1-induced tumor formation. EA.hy926 cells transduced with K1, Tat, or both were s.c. injected into the left flanks of nude mice to induce tumors. We found that K1 and Tat synergized with each other to induce faster tumor progression than the K1 or Tat alone. At day 36 post-inoculation, tumors were observed in all the mice inoculated with cells containing both Tat and K1 while only 40% of mice inoculated with cells containing either K1 or Tat alone developed tumors (Figure 5A). Tumor volumes in the K1 and Tat group grew significantly faster than those of K1 or Tat alone groups (Figure 5B). At day 64 post-inoculation when all the mice were sacrificed, the tumors from the K1 and Tat group were significantly heavier and larger than those of the K1 or Tat alone group (Figure 5C and D). H&E staining of tumor tissues showed that there were more and bigger sizes of blood vessels, and more obvious inflammatory infiltration in the K1 and Tat group than the Tat or

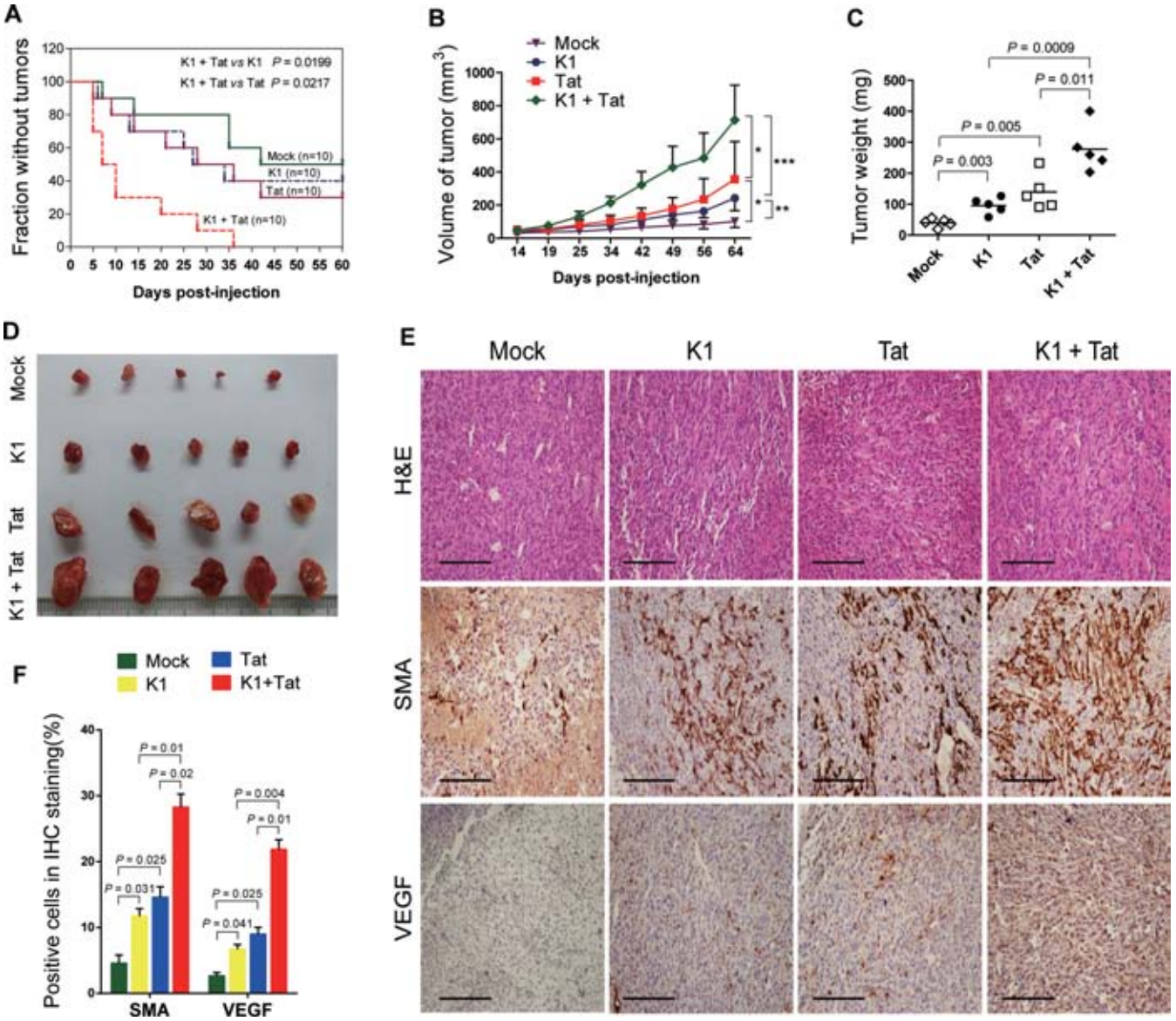

Figure 5. Tat promotes tumorigenesis induced by K1 in nude mice. (**A**) Kaplan–Meier plot of tumorigenesis in nude mice. EA.hy926 cells transduced by K1, Tat or both were sc injected into the left flanks of nude mice. The palpable tumor appearances of mice were daily monitored for 60 days. (**B**) Tumor size induced by K1 with synergistic promotion by Tat, measured by Vernier caliper. Data represent mean ± SD. $n = 5$ tumors per group. Two independent experiments were performed and gave similar results. $^{*}P < 0.05$, $^{**}P < 0.01$ and $^{***}P < 0.001$. (**C**) Tumor weight induced by K1 with synergistic promotion from Tat. Nude mice that treated as in (A) were sacrificed at days 64; tumor tissue was harvested and weighed immediately. Data represent mean ± SD, each group with five tumors. Two independent experiments were performed and similar results were obtained. (**D**) Photographs of harvested tumors. (**E**) H&E staining of tumor tissue (top; ×200) and immunohistochemical staining of SMA and VEGF (middle and bottom; ×200). (**F**). Quantitative scanning of SMA and VEGF expression of the results in (E).

K1 alone group (Figure 5E). Tumors from the K1 and Tat group also had more cells that were positive for SMA and VEGF with stronger staining than those of the K1 or Tat alone group (Figure 5E and F). These results collectively indicate that Tat promotes K1-induced tumor formation in nude mice.

Western blotting of the tumor tissues from nude mice demonstrated that the K1 and Tat group had IκBα expression lower than that of K1 or Tat alone group (Figure 6A). As expect, Tat or K1 alone increased the level of phosphorylated p65, and Tat and K1 further manifested synergistic effect to increase the level of phosphorylated p65 (Figure 6A). Consistently, immunohistochemical staining revealed a higher level of phosphorylated p65 in the K1 and Tat group than that of the K1 or Tat alone group (Figure 6B and C). To examine the role of the NF-κB pathway in the synergistic tumor-inducing effects of Tat and K1, we tested the effect of the NF-κB inhibitor Bay11–7082 on tumor growth. Bay11–7082 was administrated intraperitoneally into the nude mice every 2 days for a total of five times when tumors reached similar sizes (80–100 mm^3) at day 14 post-inoculation for all the groups. Bay11–7082 significantly inhibited the growth of tumors in all groups. There was no statistically significance among the tumor sizes from all the

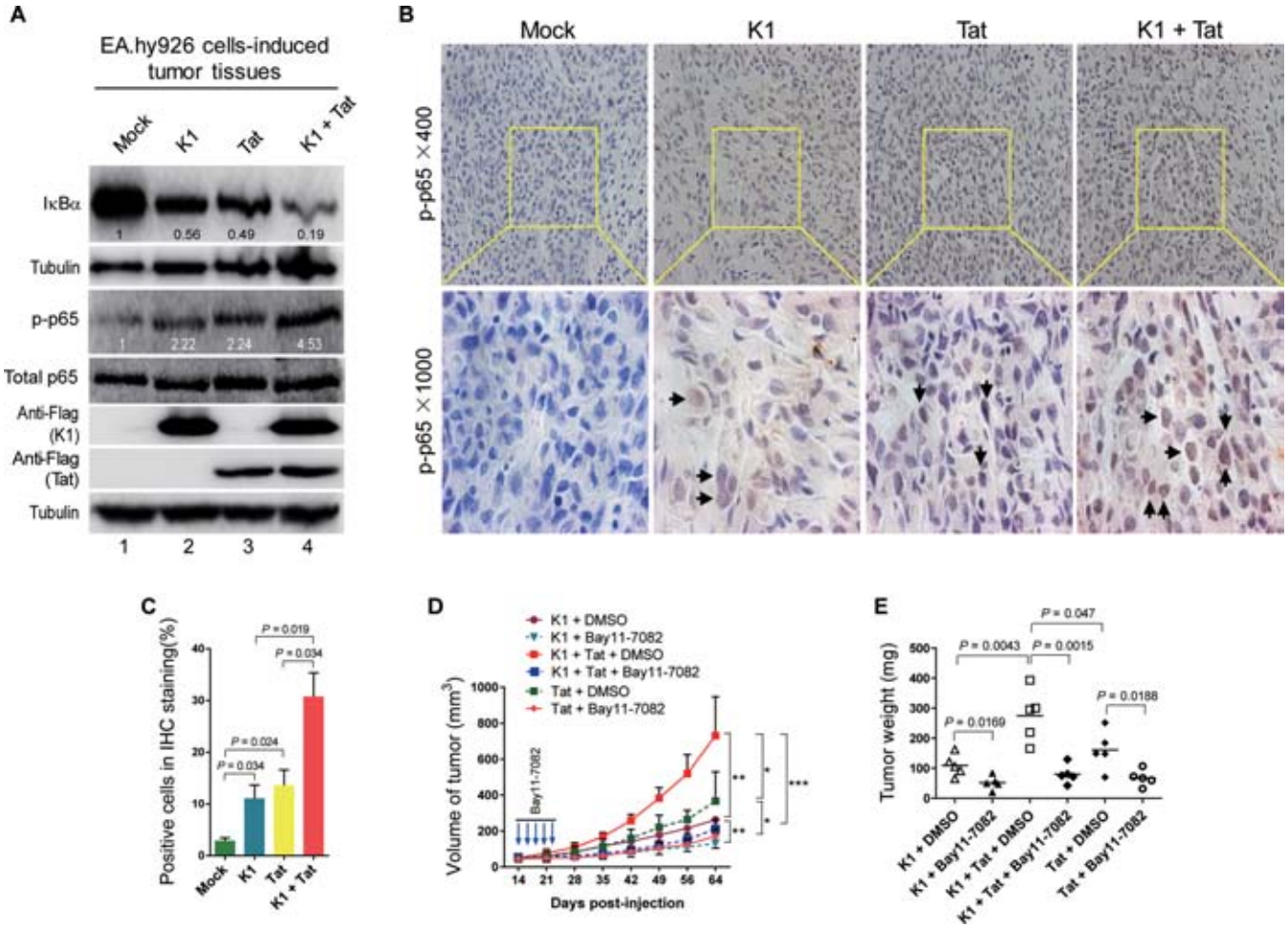

Figure 6. Tat synergizes with K1 to promote tumorigenesis in nude mice by activating the NF-κB pathway. (**A**) Expression of IκBα, phosphorylated p65 and total p65 in tumor tissue of nude mice. EA.hy926 cells transduced by K1, Tat or both were injected (s.c.) into the left flanks of nude mice. The tumor was isolated at days 64 and subject to Western blotting for IκBα expression. (**B**) Immunohistochemical staining of phosphorylated p65 in cell nucleus of tumor tissues of nude mice. EA.hy926 cells were treated as in (A) and the tumor tissue was fixed in formalin, and embedded in paraffin for immunohistochemical detection of nuclear translocation of NF-κB p65. Black arrows point to phosphorylated p65 staining in cell nucleus. (**C**) Quantitative scanning of phosphorylated p65 nuclear translocation of the results in (B). (**D**) Activation of NF-κB is required for Tat promotion of K1-induced tumorigenesis indicated by tumor size. EA.hy926 cells transduced with K1 and Tat were injected (s.c.) into the left flanks of mice for xenograft formation. The mice received the treatments by intraperitoneal injection of Bay11–7082. The results are expressed as the mean ± SD, each group with five tumors. Two independent experiments were performed and similar results were obtained. (**E**) Weight of tumors isolated in (D), five tumors per group, presented as mean ± SD.

groups treated with the inhibitor at the end of the study (Figure 6D). Bay11–7082 also significantly reduced the tumor weight in all groups. The weights of tumors from all groups treated with Bay11–708 were similar (Figure 6E).

Together these data suggest that Tat synergizes with K1 to induce angiogenesis and tumorigenesis through activation of the NF-κB pathway.

Cellular miR-891a-5p directly targets IκBα

The above results showed that inhibition of IκBα might contribute to the synergy between Tat and K1 in promoting angiogenesis and tumorigenesis. Since K1 and Tat affected IκBα protein level, we next asked whether K1 and Tat could inhibit IκBα protein expression by down-regulating its mRNA transcript. qPCR showed that neither K1 nor Tat suppressed the expression of IκBα mRNA in EA.hy926 cells (Supplementary Figure S2). Therefore, we deduced that one or several miRNAs might regulate the IκBα function. We used miRNA microarray to screen miRNA expression in the Mock cells or cells expressing K1, Tat or both. MiRNAs in the cells expressing K1, Tat, or both with expression level >1.3 folds greater than in the Mock group were further analyzed by bioinformatics approach. Among the upregulated miRNAs in cell expressing both K1 and Tat, we predicted eight miRNAs that might have putative targeting sites in the 3′UTR of IκBα (Figure 7A). Indeed, IκBα 3′UTR luciferase reporter assay showed that miR-323a-3p, miR-421, miR-550b-3p, miR-891a-5p, miR-1284 and miR-2113 significantly inhibited the activity of IκBα 3′UTR reporter (Figure 7B). To verify the effect of these six miRNAs on the expression of the IκBα protein, miRNA mimics were transfected into HUVEC. Western blotting showed that transfection of miR-891a-5p drastically inhibited endogenous IκBα expression in HUVEC (Figure 7C). Expression of miR-891a-5p inhibited the activity of IκBα

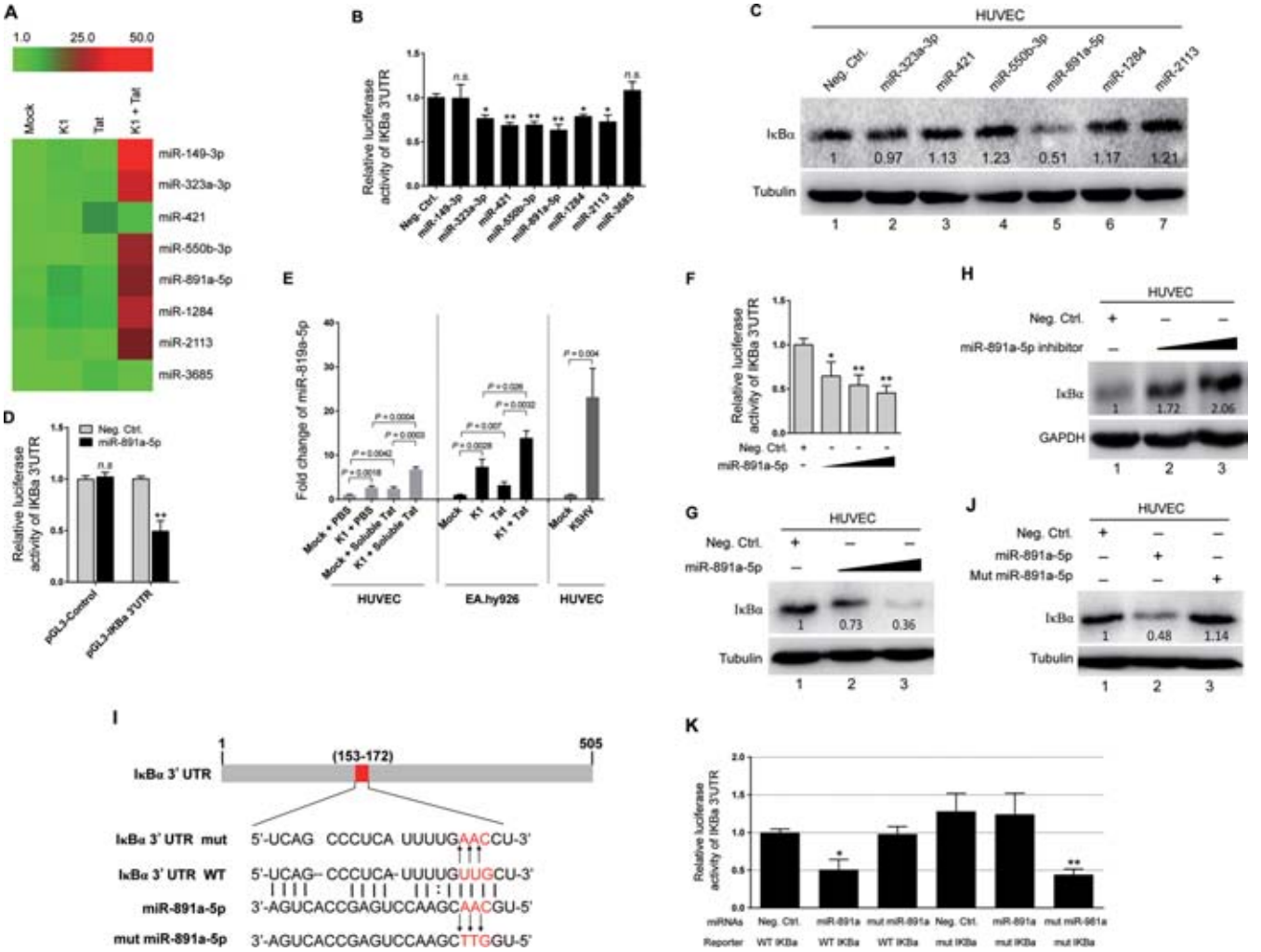

Figure 7. miR-891a-5p regulates NF-κB pathway by targeting IκBα 3′UTR. (**A**) Thermal analysis of eight miRNAs with differential expression levels in EA.hy926 cells transduced with K1, Tat or both, which were predicted to target IκBα 3′UTR through bioinformatics approach. The color scale from green to red represents low to high expression intensity of miRNAs. (**B**) Inhibition of IκBα 3′UTR reporter activity by miRNAs. HEK293T cells were co-transfected with miRNA mimics (10 nM) predicted in (A) or miRNA negative control (Neg. Ctrl.) together with pGL3-IκBα 3′UTR luciferase reporter and assayed for luciferase activity. The data represent the mean ± SEM from three independent experiments ($n = 3$), each experiment containing four technical replicates. $*P < 0.05$ and $**P < 0.01$; n.s. not significant. (**C**) The influence of miRNAs on expression of endogenous IκBα. HUVEC transfected with miRNA mimics (20 nM) and negative control were subject to western blotting at 48 h post-transfection. (**D**) miR-891a-5p inhibited the reporter activity of the pGL-3-IκBα 3′UTR but not the control reporter pGL3. miR-891a-5p mimics (50 nM) or negative control with pGL3-Control or pGL-3-IκBα 3′UTR reporter plasmid were co-transfected into HEK293T cells for 48 h. $**P < 0.01$ by Student's *t* test versus the Neg. Ctrl. group. n.s., not significant. (**E**) RT-qPCR detection of miR-891a-5p expression in K1-transduced HUVEC at 72 h after adding soluble Tat (left); in EA.hy926 cells with ectopic expression of Tat (middle); and in HUVEC infected by KSHV (BAC16) (right). (**F**) miR-891a-5p mimics (10, 20 and 50 nM) or a negative control were co-transfected into HEK293T cells along with pGL-3-IκBα 3′UTR reporter plasmid. Luciferase assay was performed 48 h later. Results were verified in three independently repeated experiments ($n = 3$) with four technical replicates, presented as mean ± SEM. $*P < 0.05$ and $**P < 0.01$ by Student's *t* test versus the Neg. Ctrl. group. (**G**) miR-891a-5p inhibited expression of endogenous IκBα in a dose-dependent manner. miR-891a-5p mimics (10 and 50 nM) were transfected into HUVEC and Western blotting was performed with anti-IκBα antibody at 48 h post-transfection. (**H**) Inhibition of miR-891a-5p promoted expression of endogenous IκBα. miR-891a-5p inhibitor (10 and 50 nM) were transfected into HUVEC and western blotting was performed with anti-IκBα antibody at 48 h post-transfection. (**I**) Schematic diagram of predicted seed sequence of miR-891a-5p which binds with IκBα 3′UTR, and mutation of the binding site of miR-891a-5p or IκBα 3′UTR. (**J**) miR-891a-5p mutant without the sequence binding to IκBα 3′UTR lost its inhibitory effect on IκBα expression. miR-891a-5p mimics (20 nM), miR-891a-5p mutant and a negative control were transfected into HUVEC and Western blotting was performed with anti-IκBα antibody at 48 h post-transfection. (**K**). Effect of seed mutagenesis or mutation of the binding site on the IκBα 3′UTR reporter. IκBα 3′UTR wild type (WT IκBα) was co-transfected with a negative control (Neg. Ctrl.), natural (miR-891a-5p) or mutant miR-891a-5p (mut miR-891a-5p) into HEK293T cells, while mutant IκBα 3′UTR construct (mut IκBα) was also co-transfected with a negative control (Neg. Ctrl.), natural (miR-891a-5p) or mutant miR-891a-5p (mut miR-891a-5p). After co-transfection for 48 h, HEK293T cells were assayed for luciferase activity. The data represent the mean ± SEM from three independent experiments ($n = 3$), each experiment containing four technical replicates. $*P < 0.05$ and $**P < 0.01$ by Student's *t*-test.

3′UTR reporter but not that of the control reporter (Figure 7D). RT-qPCR confirmed that Tat, K1 or both indeed increased the expression of miR-891a-5p in both HUVEC and EA.hy926 cells with Tat and K1 manifested synergistic effect. KSHV (BAC16) infection of HUVEC also increased the level of miR-891a-5p (Figure 7E). miR-891a-5p inhibited the activity of the IκBα 3′UTR reporter and the endogenous IκBα expression in HUVEC in a dose-dependent manner (Figure 7F and G). As a result, miR-891a-5p induced the translocation of p65 (Supplementary Figure S3A), and enhanced the activity of a NF-κB reporter in a dose-dependent fashion (Supplementary Figure S3B). On the contrary, a miR-891a-5p inhibitor up-regulated the endogenous IκBα expression level and inhibited the activity of a NF-κB reporter in HUVEC in a dose-dependent manner (Figure 7H and Supplementary Figure S3C). Bioinformatics analysis identified one putative miR-891a-5p binding site in the IκBα 3′UTR (Figure 7I). Mutation of this site abolished the miR-891a-5p inhibitory effect on endogenous IκBα expression (Figure 7J) and IκBα 3′UTR reporter activity (Figure 7K) in HUVEC cells. These data suggest that miR-891a-5p directly targets IκBα.

miR-891a-5p mediates K1- and Tat-induced angiogenesis by targeting IκBα to activate the NF-κB pathway

To evaluate the effect of inhibiting miR-891a-5p on K1- and Tat-induced angiogenesis, we constructed a lentivirus expressing a miR-891a-5p sponge. The miR-891a-5p sponge inhibited single cell colony formation induced by K1, Tat or both (Figure 8A and B). Tubule formation assay was performed with HUVEC transduced with K1, incubated with soluble Tat protein or subjected to both treatments, and co-transfected with an inhibitor of miR-891a-5p or a scrambled control. The miRNA suppressor of miR-891a-5p blocked tubule formation of HUVEC induced by K1, Tat or both (Figure 8C and D). Western blotting showed that the miR-891a-5p inhibitor indeed relieved the degradation of IκBα exerted by miR-891a-5p (elevated expression in lanes 2, 4 and 6 in Figure 8E).

Finally, we examined the effect of miR-891a-5p on K1- and Tat-induced angiogenesis *in vivo*. HUVEC transduced with K1, incubated with soluble Tat alone or both were transfected with the miR-891a-5p inhibitor and subsequently implanted onto CAMs. Consistent with the *in vitro* results, inhibition of the function of miR-891a-5p suppressed angiogenic effect induced by K1, Tat or both (Figure 9A and B). Similar results were also observed in the Matrigel plug assay (Figure 9C and D). ELISA results showed that the miR-891a-5p sponge decreased the activity of p65 binding to the NF-κB consensus site in the tumor tissues isolated from Matrigel plug assay (Figure 9E). Consistent with these observations, Western blotting showed that the miR-891a-5p sponge inhibited IκBα degradation in the plug tumor tissues induced by K1, Tat or both in EA.hy926 cells (lanes 2, 4, 6 showed elevated expression of IκBα protein in Figure 9F). Together these data suggest that miR-891a-5p mediates K1- and Tat-induced angiogenesis by targeting IκBα to activate the NF-κB pathway.

DISCUSSION

KS is a malignant tumor characterized by abnormal growth of blood vessels. AIDS-KS, in particular, is aggressive and difficult to treat (3,36,52). By encoding viral oncogenes, KSHV induces the development of KS through a complex tumorigenic mechanism. The current study focused on Orf-K1, which has been detected in the tissues of KS, PEL and MCD (10,12,53). As a multifunctional tumorigenic protein expressed at the early lytic stage of KSHV infection, K1 exerts its function in the pathogenesis of KS by regulating cellular signaling and inducing growth and angiogenic factors, and inflammatory cytokines. On the other hand, in AIDS-KS, HIV-1 can also promote the oncogenic process of KSHV through auxiliary proteins, such as Tat and Nef. For instance, HIV-1 Tat sensitizes the JAK/STAT pathway and activates the PI3K/Akt and NF-κB pathways to regulate KSHV replication and accelerate KSHV tumorigenesis (22,33,35,40). Tat also induces the secretion of cytokines such as VEGF and b-FGF, and activates VEGFR2 (22,23,33–35,48,54–58). Therefore, Tat is a promoting factor of AIDS-KS albeit itself is not sufficient to cause KS (9).

In this study, we found that, as an independent factor, Tat or K1 not only promoted cell proliferation, plate colony formation and endothelial cell microtubule formation, but also enhanced angiogenesis in CAM and nude mice models, which was consistent with results of previous studies (10,13–15,22,38). Further, Tat synergized with K1 to promote the angiogenesis in endothelial cells. Both VEGF and b-FGF promote angiogenesis in AIDS-KS patients (9,17). Since NF-κB and PI3K/AKT pathways are the two key pathways that regulate the secretions of VEGF and b-FGF (6,59), in this study, we investigated the signaling molecules of these pathways. We showed that Tat drastically reduced the IκBα level in K1-transduced cells, and activated the NF-κB signaling. Immunohistochemistry confirmed the nuclear translocation of cytosolic p65, which promoted the transcription and expression of angiogenesis-related genes, such as VEGF. As uptake of Tat by cells is very efficient (60,61), Tat is detected in spindle cells of AIDS-KS lesions (32), and HIV-1-infected patients often have a high level of circulating Tat (26), we believe that our observations are highly relevant to the clinical setting.

A few of the KSHV oncogenes can activate the NF-κB pathway, including vFLIP (Orf-K13), Orf-K15 and vGPCR (Orf74) (62–66). Induction of tumor formation by vFLIP and vGPCR depends on the activation of NF-κB pathway. On the other hand, the vIRF-3 (Orf-K10.5) inhibits IKKβ activation, resulting in the inhibition of the immunoregulatory function of the NF-κB pathway (67). Here, we showed that Orf-K1 suppressed IκBα expression and activated the NF-κB pathway to induce angiogenesis, which was synergistically enhanced by Tat. However, Konrad and colleagues used reverse-transfected cell microarrays to observe the interaction between different oncogenic proteins, and found that K1 inhibited vFLIP and ORF75-activated NF-κB pathway (68). Orf-K1 also inhibited TPA-activated NF-κB signaling in PEL cell line, leading to the suppression of viral replication (69). It is worth mentioning that different cell lines were used in these studies. Thus, Orf-K1 might

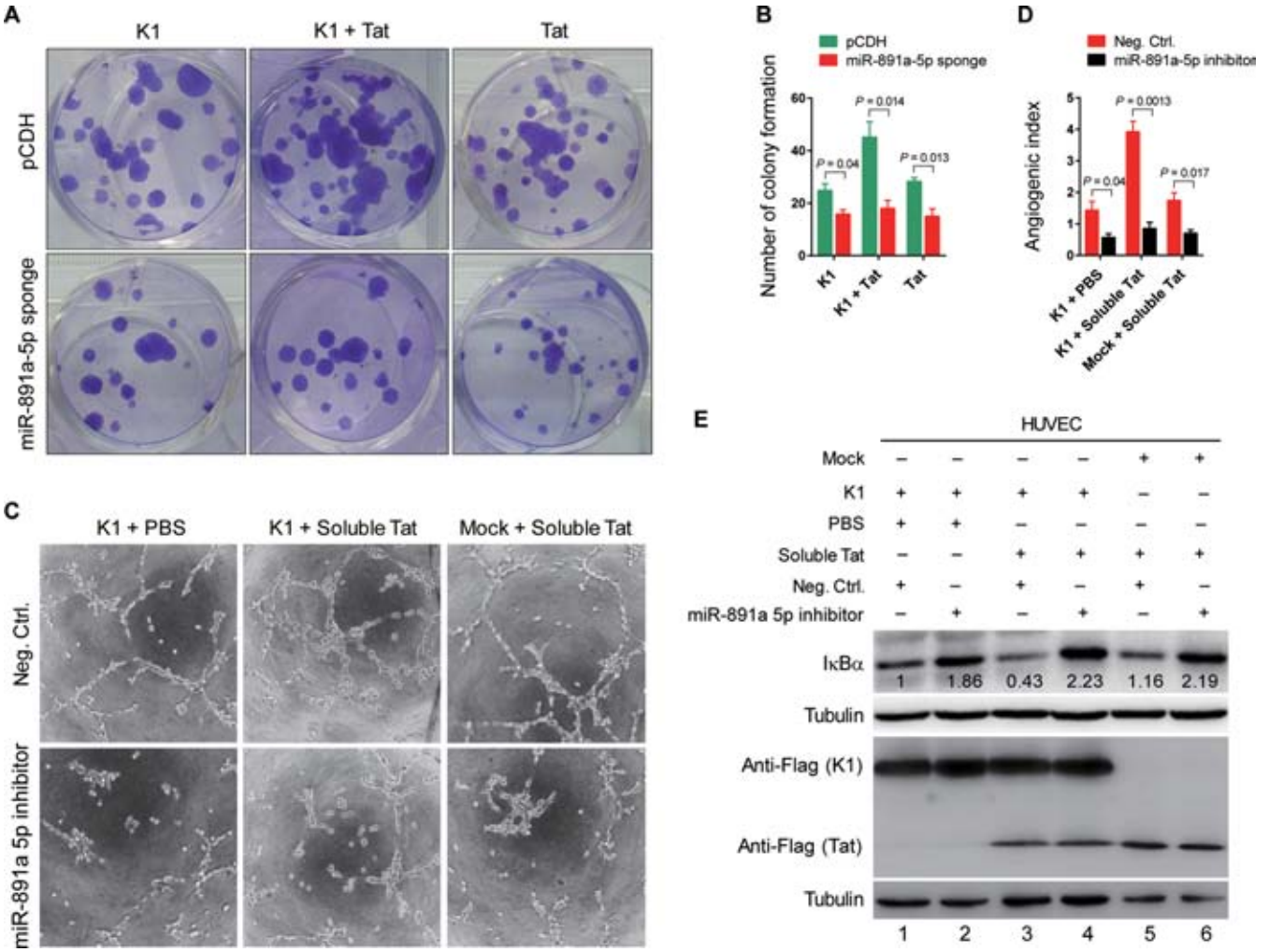

Figure 8. Inhibition of miR-891a-5p suppresses the synergistic promotion of Tat- and K1-induced cell proliferation and microtubule formation by inhibiting NF-κB pathway. (**A**) Plate colony formation assay to measure the influence of miR-891a-5p sponge on synergistic promotion of Tat- and K1-induced colony formation. EA.hy926 cells transduced with K1, Tat and both were further transduced with lentivial miR-891a-5p sponge or its control pCDH. Cells were seeded and stained with crystal violet 14 days later to evaluate the size and number of clones formed. (**B**) Quantification of the results in (A). The data represent the mean ± SEM from three independent experiments ($n = 3$), each experiment containing six technical replicates. (**C**) Microtubule formation assay to measure the influence of miR-891a-5p inhibitor on synergistic promotion of Tat- and K1-induced microtubule formation. HUVEC transduced with K1 or incubated with soluble Tat were transfected with miR-891a-5p inhibitor and a negative control. Cells were then seeded onto plates with Matrigel and photographed under a microscope (×100) after 16 h. (**D**) Quantification of the results in (C). The data represent the mean ± SEM from three independent experiments ($n = 3$), each experiment containing six technical replicates. (**E**) Inhibition of miR-891a-5p elevated IκBα *in vitro*. Western blotting was performed to examine IκBα expression in cells treated as described in (C).

regulate NF-κB signaling to mediate host cell proliferation and tumorigenesis through distinct mechanisms depending on cell context (69). Our results and those of other studies have demonstrated that K1 mediates KS development through the activation of NF-κB signaling (4,53,59). During KSHV latency, the NF-κB pathway in KS and PEL is constitutively activated, which inhibits viral replication to promote latent infection (70–73). This strategy effectively protects the infected cells from apoptosis, evades host immune clearance, and provides an appropriate microenvironment for KS tumor growth through the expression of inflammation-related angiogenic factors such as VEGF, IL-6 and TNF-α (6,71,74). More importantly, in KS tumors, a small number of tumors express KSHV lytic genes, such as K1, K15 and vGPCR to activate the NF-κB pathway, and promote KS development (4,5,13,17,66,75). Therefore, the NF-κB pathway might be a converging pathway of both latent infection and lytic replication that is essential for the development of KS.

miRNAs are small RNAs with a length of 21–23 nucleotides, which post-transcriptionally regulate the expression of genes by targeting their 3′UTRs. Thus, it has become a molecular target in tumor diagnosis and treatment (76,77). With respect to miRNAs and IκBα, to date, three cellular miRNAs including miR-126, miR-30e* and miR-196a, and KSHV miR-K1 have been identified to directly target IκBα 3′UTR. The cellular miRNAs increase the occurrence of ulcer disease, glioma, and pancreatic cancer, respectively, while miR-K1 promotes KSHV latency and enhances cell growth and survival (41,78–81). In this study,

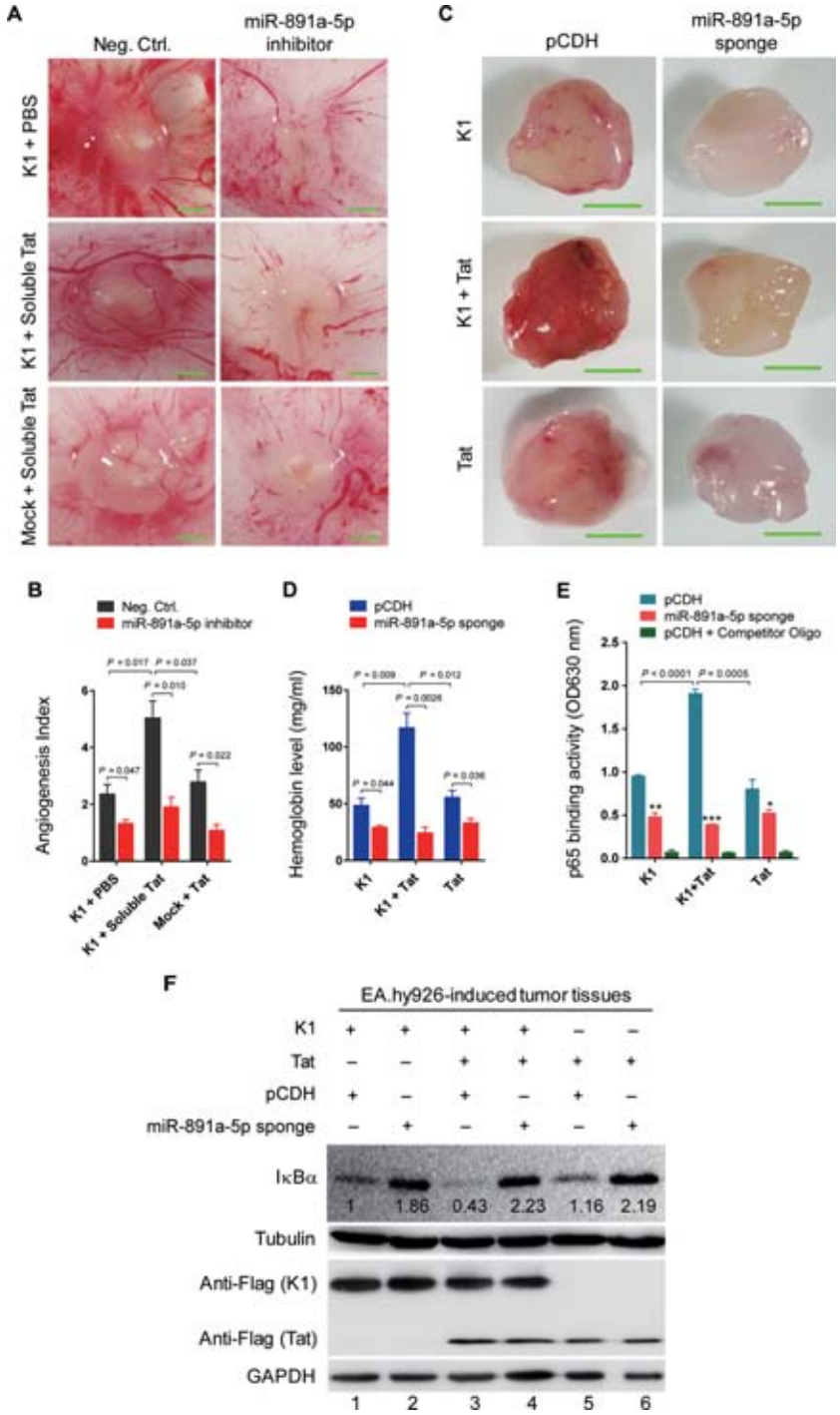

Figure 9. Inhibition of miR-891a-5p suppresses the synergistic promotion of Tat- and K1-induced angiogenesis in animal models by inhibiting NF-κB pathway. (**A**) Inhibitory effect of miR-891a-5p inhibitor on synergistic promotion of Tat- and K1-induced angiogenesis in CAM model. HUVEC transduced with K1 or incubated with Tat were transfected with miR-891a-5p inhibitor or a negative control and further implanted into CAM model. CAMs were harvested 4 days later; vessels were observed by stereomicroscopy; and representative photographs were taken. (**B**) Quantification of the results in (A). The number of blood vessels was normalized to that of Matrigel alone. Data represent mean ± SEM from three independent experiments ($n = 3$), each experiment containing six technical replicates. (**C**) Inhibitory effect of miR-891a-5p sponge on synergistic promotion of Tat- and K1-induced angiogenesis in nude mice. EA.hy926 cells transduced by K1, Tat or both were transduced with lentiviral miR-891a-5p sponge or its control pCDH, and further examined for their proangiogenic effects in Matrigel plug assay in nude mice. Representative photographs of angiogenesis in the nude mice are shown. (**D**) The hemoglobin level of the Matrigel plug treated as in (C) was determined with hemoglobin content calculated based on the standard curve. Data represent mean ± SEM determined from three independent experiments ($n = 3$), each experiment containing six technical replicates. (**E**) NF-κB p65–DNA binding activity assay. Nuclear proteins were extracted from plug tissues of nude mice treated as described in (C), followed by determination of ELISA. Data represent mean ± SEM determined from three independent experiments ($n = 3$), each experiment containing three technical replicates. Compared with competitive oligonucleotide: $^{*}P < 0.05$, $^{**}P < 0.01$ and $^{***}P < 0.001$. (**F**) Western blotting analysis of IκBα in plug tissues from nude mice treated as in (C).

high expression of miR-891a-5p was observed in Orf-K1 and Tat-transduced cells. We have shown that miR-891a-5p also directly targets IκBα 3′UTR. The synergistic promotion of endothelial cell proliferation and angiogenesis by Tat and K1 was markedly inhibited by miR-891a-5p inhibitor or its sponge *in vitro* and *in vivo*, which were consistent with the inhibition of IκBα expression. These results revealed that Tat synergized with Orf-K1 to down-regulate IκBα expression, resulting in increased nuclear translocation of p65, activation of the NF-κB pathway and enhanced angiogenesis through up-regulating miR-891a-5p. Importantly, high miR-891a-5p expression was also detected in KSHV-infected HUVEC. Recent studies have shown that sera from EBV-related nasopharyngeal carcinoma (NPC) patients have high levels of miR-891a-5p in the exosomes (82). Interestingly, miR-891a-5p can also increase the migration of SK-HEP-1 hepatocellular carcinoma cells (83). Taken together, miR-891a-5p appears to be a pro-angiogenic and pro-tumorigenic miRNA.

In summary, our results reveal that miR-891a-5p mediates the synergy between Tat and Orf-K1 in the induction of angiogenesis by targeting IκBα and activating the NF-κB pathway. Our study illustrated a mechanism by which a HIV-1 secreted protein synergistically facilitates KSHV oncogenic protein-induced angiogenesis in AIDS-KS patients through the miR-891a-5p/NF-κB/VEGF pathway. It would be worthwhile to examine the therapeutic effect of targeting this pathway in AIDS-KS. Further investigations are needed to explore the mechanism by which Tat and K1 regulate the expression of miR-891a-5p, and whether other cellular miRNAs might also regulate Tat- and K1-induced angiogenesis.

SUPPLEMENTARY DATA

Supplementary Data are available at NAR Online.

ACKNOWLEDGEMENTS

We are grateful to members from Dr Lu laboratory for helpful discussion.
Author Contributions: Conceived and designed the experiments: Q.Y., C.L. Performed the experiments: S.Y., M.H., T.H., W.L., X.X., M.X. Provided the reagents: S.J.G. Analyzed the data: X.Z., F.Z., D.Q., Q.Y., J.Z., S.J.G., C.L. Wrote the paper: Q.Y., S.J.G., C.L.

FUNDING

National Natural Science Foundation of China [81361120387, 81371824, 81171552, 31270199, 81401662, 81571984]; NIH [R01CA177377, R01CA132637]; Ph.D. Programs Foundation of Ministry of Education of China [20123234110006]; Natural Science Youth Foundation of Jiangsu Province [BK20140908]; Quzhou Science and Technology Bureau (2013Y020). Funding for open access charge: National Natural Science Foundation of China.
Conflict of interest statement. None declared.

REFERENCES

1. Chang,Y., Cesarman,E., Pessin,M.S., Lee,F., Culpepper,J., Knowles,D.M. and Moore,P.S. (1994) Identification of herpesvirus-like DNA sequences in AIDS-associated Kaposi's sarcoma. *Science*, **266**, 1865–1869.
2. Ganem,D. (2006) KSHV infection and the pathogenesis of Kaposi's sarcoma. *Annu. Rev. Pathol.*, **1**, 273–296.
3. Cai,Q., Verma,S.C., Lu,J. and Robertson,E.S. (2010) Molecular biology of Kaposi's sarcoma-associated herpesvirus and related oncogenesis. *Adv. Virus Res.*, **78**, 87–142.
4. Mesri,E.A., Cesarman,E. and Boshoff,C. (2010) Kaposi's sarcoma and its associated herpesvirus. *Nat. Rev. Cancer*, **10**, 707–719.
5. Cousins,E. and Nicholas,J. (2014) Molecular biology of human herpesvirus 8: novel functions and virus-host interactions implicated in viral pathogenesis and replication. *Recent Results Cancer Res.*, **193**, 227–268.
6. Dai,L., Bratoeva,M., Toole,B.P., Qin,Z. and Parsons,C. (2012) KSHV activation of VEGF secretion and invasion for endothelial cells is mediated through viral upregulation of emmprin-induced signal transduction. *Int. J. Cancer*, **131**, 834–843.
7. Aoki,Y. and Tosato,G. (2001) Vascular endothelial growth factor/vascular permeability factor in the pathogenesis of primary effusion lymphomas. *Leuk. Lymphoma*, **41**, 229–237.
8. Samaniego,F., Markham,P.D., Gendelman,R., Watanabe,Y., Kao,V., Kowalski,K., Sonnabend,J.A., Pintus,A., Gallo,R.C. and Ensoli,B. (1998) Vascular endothelial growth factor and basic fibroblast growth factor present in Kaposi's sarcoma (KS) are induced by inflammatory cytokines and synergize to promote vascular permeability and KS lesion development. *Am. J. Pathol.*, **152**, 1433–1443.
9. Barillari,G., Sgadari,C., Palladino,C., Gendelman,R., Caputo,A., Morris,C.B., Nair,B.C., Markham,P., Nel,A., Sturzl,M. *et al.* (1999) Inflammatory cytokines synergize with the HIV-1 Tat protein to promote angiogenesis and Kaposi's sarcoma via induction of basic fibroblast growth factor and the alpha v beta 3 integrin. *J. Immunol.*, **163**, 1929–1935.
10. Wang,L., Dittmer,D.P., Tomlinson,C.C., Fakhari,F.D. and Damania,B. (2006) Immortalization of primary endothelial cells by the K1 protein of Kaposi's sarcoma-associated herpesvirus. *Cancer Res.*, **66**, 3658–3666.
11. Lagunoff,M., Majeti,R., Weiss,A. and Ganem,D. (1999) Deregulated signal transduction by the K1 gene product of Kaposi's sarcoma-associated herpesvirus. *Proc. Natl. Acad. Sci. U.S.A.*, **96**, 5704–5709.
12. Lee,B.S., Connole,M., Tang,Z., Harris,N.L. and Jung,J.U. (2003) Structural analysis of the Kaposi's sarcoma-associated herpesvirus K1 protein. *J. Virol.*, **77**, 8072–8086.
13. Wang,L., Wakisaka,N., Tomlinson,C.C., DeWire,S.M., Krall,S., Pagano,J.S. and Damania,B. (2004) The Kaposi's sarcoma-associated herpesvirus (KSHV/HHV-8) K1 protein induces expression of angiogenic and invasion factors. *Cancer Res.*, **64**, 2774–2781.
14. Wang,L. and Damania,B. (2008) Kaposi's sarcoma-associated herpesvirus confers a survival advantage to endothelial cells. *Cancer Res.*, **68**, 4640–4648.
15. Lee,H., Veazey,R., Williams,K., Li,M., Guo,J., Neipel,F., Fleckenstein,B., Lackner,A., Desrosiers,R.C. and Jung,J.U. (1998) Deregulation of cell growth by the K1 gene of Kaposi's sarcoma-associated herpesvirus. *Nat Med*, **4**, 435–440.
16. Bhatt,A.P. and Damania,B. (2012) AKTivation of PI3K/AKT/mTOR signaling pathway by KSHV. *Front. Immunol*, **3**, 401.
17. Guilluy,C., Zhang,Z., Bhende,P.M., Sharek,L., Wang,L., Burridge,K. and Damania,B. (2011) Latent KSHV infection increases the vascular permeability of human endothelial cells. *Blood*, **118**, 5344–5354.
18. Mercader,M., Taddeo,B., Panella,J.R., Chandran,B., Nickoloff,B.J. and Foreman,K.E. (2000) Induction of HHV-8 lytic cycle replication by inflammatory cytokines produced by HIV-1-infected T cells. *Am. J. Pathol.*, **156**, 1961–1971.
19. Morris,A.K. and Valley,A.W. (1996) Overview of the management of AIDS-related Kaposi's sarcoma. *Ann. Pharmacother.*, **30**, 1150–1163.
20. Ensoli,B., Barillari,G., Salahuddin,S.Z., Gallo,R.C. and Wong-Staal,F. (1990) Tat protein of HIV-1 stimulates growth of cells derived from Kaposi's sarcoma lesions of AIDS patients. *Nature*, **345**, 84–86.
21. Zhu,X., Guo,Y., Yao,S., Yan,Q., Xue,M., Hao,T., Zhou,F., Zhu,J., Qin,D. and Lu,C. (2014) Synergy between Kaposi's sarcoma-associated herpesvirus (KSHV) vIL-6 and HIV-1 Nef

protein in promotion of angiogenesis and oncogenesis: role of the AKT signaling pathway. *Oncogene*, **33**, 1986–1996.
22. Zhou,F., Xue,M., Qin,D., Zhu,X., Wang,C., Zhu,J., Hao,T., Cheng,L., Chen,X., Bai,Z. *et al.* (2013) HIV-1 Tat Promotes Kaposi's Sarcoma-Associated Herpesvirus (KSHV) vIL-6-Induced Angiogenesis and Tumorigenesis by Regulating PI3K/PTEN/AKT/GSK-3beta Signaling Pathway. *PLoS One*, **8**, e53145.
23. Aoki,Y. and Tosato,G. (2007) Interactions between HIV-1 Tat and KSHV. *Curr. Top. Microbiol. Immunol.*, **312**, 309–326.
24. Qiao,X., He,B., Chiu,A., Knowles,D.M., Chadburn,A. and Cerutti,A. (2006) Human immunodeficiency virus 1 Nef suppresses CD40-dependent immunoglobulin class switching in bystander B cells. *Nat. Immunol.*, **7**, 302–310.
25. Li,J.C., Yim,H.C. and Lau,A.S. (2010) Role of HIV-1 Tat in AIDS pathogenesis: its effects on cytokine dysregulation and contributions to the pathogenesis of opportunistic infection. *AIDS*, **24**, 1609–1623.
26. Cafaro,A., Caputo,A., Fracasso,C., Maggiorella,M.T., Goletti,D., Baroncelli,S., Pace,M., Sernicola,L., Koanga-Mogtomo,M.L., Betti,M. *et al.* (1999) Control of SHIV-89.6P-infection of cynomolgus monkeys by HIV-1 Tat protein vaccine. *Nat. Med.*, **5**, 643–650.
27. Huigen,M.C., Kamp,W. and Nottet,H.S. (2004) Multiple effects of HIV-1 trans-activator protein on the pathogenesis of HIV-1 infection. *Eur. J. Clin. Invest.*, **34**, 57–66.
28. Faller,E.M., Sugden,S.M., McVey,M.J., Kakal,J.A. and MacPherson,P.A. (2010) Soluble HIV Tat protein removes the IL-7 receptor alpha-chain from the surface of resting CD8 T cells and targets it for degradation. *J. Immunol.*, **185**, 2854–2866.
29. Chang,H.C., Samaniego,F., Nair,B.C., Buonaguro,L. and Ensoli,B. (1997) HIV-1 Tat protein exits from cells via a leaderless secretory pathway and binds to extracellular matrix-associated heparan sulfate proteoglycans through its basic region. *AIDS*, **11**, 1421–1431.
30. Wood,N.H. and Feller,L. (2008) The malignant potential of HIV-associated Kaposi sarcoma. *Cancer Cell Int.*, **8**, 14.
31. Rusnati,M. and Presta,M. (2002) HIV-1 Tat protein and endothelium: from protein/cell interaction to AIDS-associated pathologies. *Angiogenesis*, **5**, 141–151.
32. Ensoli,B., Gendelman,R., Markham,P., Fiorelli,V., Colombini,S., Raffeld,M., Cafaro,A., Chang,H.K., Brady,J.N. and Gallo,R.C. (1994) Synergy between basic fibroblast growth factor and HIV-1 Tat protein in induction of Kaposi's sarcoma. *Nature*, **371**, 674–680.
33. Zeng,Y., Zhang,X., Huang,Z., Cheng,L., Yao,S., Qin,D., Chen,X., Tang,Q., Lv,Z., Zhang,L. *et al.* (2007) Intracellular Tat of human immunodeficiency virus type 1 activates lytic cycle replication of Kaposi's sarcoma-associated herpesvirus: role of JAK/STAT signaling. *J. Virol.*, **81**, 2401–2417.
34. Guo,H.G., Pati,S., Sadowska,M., Charurat,M. and Reitz,M. (2004) Tumorigenesis by human herpesvirus 8 vGPCR is accelerated by human immunodeficiency virus type 1 Tat. *J. Virol.*, **78**, 9336–9342.
35. Chen,X., Cheng,L., Jia,X., Zeng,Y., Yao,S., Lv,Z., Qin,D., Fang,X., Lei,Y. and Lu,C. (2009) Human immunodeficiency virus type 1 Tat accelerates Kaposi sarcoma-associated herpesvirus Kaposin A-mediated tumorigenesis of transformed fibroblasts in vitro as well as in nude and immunocompetent mice. *Neoplasia*, **11**, 1272–1284.
36. Barillari,G. and Ensoli,B. (2002) Angiogenic effects of extracellular human immunodeficiency virus type 1 Tat protein and its role in the pathogenesis of AIDS-associated Kaposi's sarcoma. *Clin. Microbiol. Rev*, **15**, 310–326.
37. Edgell,C.J., McDonald,C.C. and Graham,J.B. (1983) Permanent cell line expressing human factor VIII-related antigen established by hybridization. *Proc. Natl. Acad. Sci. U.S.A.*, **80**, 3734–3737.
38. Xue,M., Yao,S., Hu,M., Li,W., Hao,T., Zhou,F., Zhu,X., Lu,H., Qin,D., Yan,Q. *et al.* (2014) HIV-1 Nef and KSHV oncogene K1 synergistically promote angiogenesis by inducing cellular miR-718 to regulate the PTEN/AKT/mTOR signaling pathway. *Nucleic Acids Res.*, **42**, 9862–9879.
39. Wada,Y., Otu,H., Wu,S., Abid,M.R., Okada,H., Libermann,T., Kodama,T., Shih,S.C., Minami,T. and Aird,W.C. (2005) Preconditioning of primary human endothelial cells with inflammatory mediators alters the "set point" of the cell. *FASEB J.*, **19**, 1914–1916.
40. Tang,Q., Qin,D., Lv,Z., Zhu,X., Ma,X., Yan,Q., Zeng,Y., Guo,Y., Feng,N. and Lu,C. (2012) Herpes simplex virus type 2 triggers reactivation of Kaposi's sarcoma-associated herpesvirus from latency and collaborates with HIV-1 Tat. *PLoS One*, **7**, e31652.
41. Lei,X., Bai,Z., Ye,F., Xie,J., Kim,C.G., Huang,Y. and Gao,S.J. (2010) Regulation of NF-kappaB inhibitor IkappaBalpha and viral replication by a KSHV microRNA. *Nat. Cell Biol.*, **12**, 193–199.
42. Aranda,E. and Owen,G.I. (2009) A semi-quantitative assay to screen for angiogenic compounds and compounds with angiogenic potential using the EA.hy926 endothelial cell line. *Biol. Res.*, **42**, 377–389.
43. Ebert,M.S., Neilson,J.R. and Sharp,P.A. (2007) MicroRNA sponges: competitive inhibitors of small RNAs in mammalian cells. *Nat. Methods*, **4**, 721–726.
44. Yan,Q., Ma,X., Shen,C., Cao,X., Feng,N., Qin,D., Zeng,Y., Zhu,J., Gao,S.J. and Lu,C. (2014) Inhibition of Kaposi's sarcoma-associated herpesvirus lytic replication by HIV-1 Nef and cellular MicroRNA hsa-miR-1258. *J. Virol.*, **88**, 4987–5000.
45. Yan,Q., Li,W., Tang,Q., Yao,S., Lv,Z., Feng,N., Ma,X., Bai,Z., Zeng,Y., Qin,D. *et al.* (2013) Cellular microRNAs 498 and 320d regulate herpes simplex virus 1 induction of Kaposi's sarcoma-associated herpesvirus lytic replication by targeting RTA. *PLoS One*, **8**, e55832.
46. Qin,D., Feng,N., Fan,W., Ma,X., Yan,Q., Lv,Z., Zeng,Y., Zhu,J. and Lu,C. (2011) Activation of PI3K/AKT and ERK MAPK signal pathways is required for the induction of lytic cycle replication of Kaposi's sarcoma-associated herpesvirus by herpes simplex virus type 1. *BMC Microbiol.*, **11**, 240.
47. Qin,D., Zeng,Y., Qian,C., Huang,Z., Lv,Z., Cheng,L., Yao,S., Tang,Q., Chen,X. and Lu,C. (2008) Induction of lytic cycle replication of Kaposi's sarcoma-associated herpesvirus by herpes simplex virus type 1: involvement of IL-10 and IL-4. *Cell Microbiol.*, **10**, 713–728.
48. Zhu,X., Zhou,F., Qin,D., Zeng,Y., Lv,Z., Yao,S. and Lu,C. (2011) Human immunodeficiency virus type 1 induces lytic cycle replication of Kaposi's-sarcoma-associated herpesvirus: role of Ras/c-Raf/MEK1/2, PI3K/AKT, and NF-kappaB signaling pathways. *J. Mol. Biol.*, **410**, 1035–1051.
49. Kim,S., Domon-Dell,C., Kang,J., Chung,D.H., Freund,J.N. and Evers,B.M. (2004) Down-regulation of the tumor suppressor PTEN by the tumor necrosis factor-alpha/nuclear factor-kappaB (NF-kappaB)-inducing kinase/NF-kappaB pathway is linked to a default IkappaB-alpha autoregulatory loop. *J. Biol. Chem.*, **279**, 4285–4291.
50. Du,L., Wang,H., He,L., Zhang,J., Ni,B., Wang,X., Jin,H., Cahuzac,N., Mehrpour,M., Lu,Y. *et al.* (2008) CD44 is of functional importance for colorectal cancer stem cells. *Clin. Cancer Res.*, **14**, 6751–6760.
51. Keller,S.A., Hernandez-Hopkins,D., Vider,J., Ponomarev,V., Hyjek,E., Schattner,E.J. and Cesarman,E. (2006) NF-kappaB is essential for the progression of KSHV- and EBV-infected lymphomas in vivo. *Blood*, **107**, 3295–3302.
52. da Silva,S.R. and de Oliveira,D.E. (2011) HIV, EBV and KSHV: viral cooperation in the pathogenesis of human malignancies. *Cancer Lett.*, **305**, 175–185.
53. Samaniego,F., Pati,S., Karp,J.E., Prakash,O. and Bose,D. (2001) Human herpesvirus 8 K1-associated nuclear factor-kappa B-dependent promoter activity: role in Kaposi's sarcoma inflammation? *J. Natl. Cancer Inst. Monogr.*, 15–23.
54. Ray,P.E., Al-Attar,A., Liu,X.H., Das,J.R., Tassi,E. and Wellstein,A. (2014) Expression of a secreted fibroblast growth factor binding protein-1 (FGFBP1) in angioproliferative Kaposi sarcoma. *J. AIDS Clin. Res.*, **5**, 309.
55. Xu,Q., Briggs,J., Park,S., Niu,G., Kortylewski,M., Zhang,S., Gritsko,T., Turkson,J., Kay,H., Semenza,G.L. *et al.* (2005) Targeting Stat3 blocks both HIF-1 and VEGF expression induced by multiple oncogenic growth signaling pathways. *Oncogene*, **24**, 5552–5560.
56. Cavallin,L.E., Goldschmidt-Clermont,P. and Mesri,E.A. (2014) Molecular and cellular mechanisms of KSHV oncogenesis of Kaposi's sarcoma associated with HIV/AIDS. *PLoS Pathog.*, **10**, e1004154.
57. Harrington,W. Jr., Sieczkowski,L., Sosa,C., Chan-a-Sue,S., Cai,J.P., Cabral,L. and Wood,C. (1997) Activation of HHV-8 by HIV-1 tat. *Lancet*, **349**, 774–775.
58. Sui,Z., Sniderhan,L.F., Fan,S., Kazmierczak,K., Reisinger,E., Kovacs,A.D., Potash,M.J., Dewhurst,S., Gelbard,H.A. and Maggirwar,S.B. (2006) Human immunodeficiency virus-encoded Tat

activates glycogen synthase kinase-3beta to antagonize nuclear factor-kappaB survival pathway in neurons. *Eur. J. Neurosci.*, **23**, 2623–2634.
59. Prakash,O., Swamy,O.R., Peng,X., Tang,Z.Y., Li,L., Larson,J.E., Cohen,J.C., Gill,J., Farr,G., Wang,S. *et al.* (2005) Activation of Src kinase Lyn by the Kaposi sarcoma-associated herpesvirus K1 protein: implications for lymphomagenesis. *Blood*, **105**, 3987–3994.
60. Ensoli,B., Buonaguro,L., Barillari,G., Fiorelli,V., Gendelman,R., Morgan,R.A., Wingfield,P. and Gallo,R.C. (1993) Release, uptake, and effects of extracellular human immunodeficiency virus type 1 Tat protein on cell growth and viral transactivation. *J. Virol.*, **67**, 277–287.
61. Selby,M.J., Bain,E.S., Luciw,P.A. and Peterlin,B.M. (1989) Structure, sequence, and position of the stem-loop in tar determine transcriptional elongation by tat through the HIV-1 long terminal repeat. *Genes Dev.*, **3**, 547–558.
62. Field,N., Low,W., Daniels,M., Howell,S., Daviet,L., Boshoff,C. and Collins,M. (2003) KSHV vFLIP binds to IKK-gamma to activate IKK. *J. Cell Sci.*, **116**, 3721–3728.
63. Sun,Q., Matta,H., Lu,G. and Chaudhary,P.M. (2006) Induction of IL-8 expression by human herpesvirus 8 encoded vFLIP K13 via NF-kappaB activation. *Oncogene*, **25**, 2717–2726.
64. Havemeier,A., Gramolelli,S., Pietrek,M., Jochmann,R., Sturzl,M. and Schulz,T.F. (2014) Activation of NF-kappaB by the Kaposi's sarcoma-associated herpesvirus K15 protein involves recruitment of the NF-kappaB-inducing kinase, IkappaB kinases, and phosphorylation of p65. *J. Virol.*, **88**, 13161–13172.
65. Brinkmann,M.M., Glenn,M., Rainbow,L., Kieser,A., Henke-Gendo,C. and Schulz,T.F. (2003) Activation of mitogen-activated protein kinase and NF-kappaB pathways by a Kaposi's sarcoma-associated herpesvirus K15 membrane protein. *J. Virol.*, **77**, 9346–9358.
66. Pati,S., Cavrois,M., Guo,H.G., Foulke,J.S. Jr, Kim,J., Feldman,R.A. and Reitz,M. (2001) Activation of NF-kappaB by the human herpesvirus 8 chemokine receptor ORF74: evidence for a paracrine model of Kaposi's sarcoma pathogenesis. *J. Virol.*, **75**, 8660–8673.
67. Seo,T., Park,J., Lim,C. and Choe,J. (2004) Inhibition of nuclear factor kappaB activity by viral interferon regulatory factor 3 of Kaposi's sarcoma-associated herpesvirus. *Oncogene*, **23**, 6146–6155.
68. Konrad,A., Wies,E., Thurau,M., Marquardt,G., Naschberger,E., Hentschel,S., Jochmann,R., Schulz,T.F., Erfle,H., Brors,B. *et al.* (2009) A systems biology approach to identify the combination effects of human herpesvirus 8 genes on NF-kappaB activation. *J. Virol.*, **83**, 2563–2574.
69. Lee,B.S., Paulose-Murphy,M., Chung,Y.H., Connlole,M., Zeichner,S. and Jung,J.U. (2002) Suppression of tetradecanoyl phorbol acetate-induced lytic reactivation of Kaposi's sarcoma-associated herpesvirus by K1 signal transduction. *J. Virol.*, **76**, 12185–12199.
70. de Oliveira,D.E., Ballon,G. and Cesarman,E. (2010) NF-kappaB signaling modulation by EBV and KSHV. *Trends Microbiol.*, **18**, 248–257.
71. Sadagopan,S., Sharma-Walia,N., Veettil,M.V., Raghu,H., Sivakumar,R., Bottero,V. and Chandran,B. (2007) Kaposi's sarcoma-associated herpesvirus induces sustained NF-kappaB activation during de novo infection of primary human dermal microvascular endothelial cells that is essential for viral gene expression. *J. Virol.*, **81**, 3949–3968.
72. Keller,S.A., Schattner,E.J. and Cesarman,E. (2000) Inhibition of NF-kappaB induces apoptosis of KSHV-infected primary effusion lymphoma cells. *Blood*, **96**, 2537–2542.
73. Brown,H.J., Song,M.J., Deng,H., Wu,T.T., Cheng,G. and Sun,R. (2003) NF-kappaB inhibits gammaherpesvirus lytic replication. *J. Virol.*, **77**, 8532–8540.
74. Sivakumar,R., Sharma-Walia,N., Raghu,H., Veettil,M.V., Sadagopan,S., Bottero,V., Varga,L., Levine,R. and Chandran,B. (2008) Kaposi's sarcoma-associated herpesvirus induces sustained levels of vascular endothelial growth factors A and C early during in vitro infection of human microvascular dermal endothelial cells: biological implications. *J. Virol.*, **82**, 1759–1776.
75. Greene,W., Kuhne,K., Ye,F., Chen,J., Zhou,F., Lei,X. and Gao,S.J. (2007) Molecular biology of KSHV in relation to AIDS-associated oncogenesis. *Cancer Treat. Res.*, **133**, 69–127.
76. Esquela-Kerscher,A. and Slack,F.J. (2006) Oncomirs - microRNAs with a role in cancer. *Nat. Rev. Cancer*, **6**, 259–269.
77. Gregory,R.I. and Shiekhattar,R. (2005) MicroRNA biogenesis and cancer. *Cancer Res.*, **65**, 3509–3512.
78. Feng,X., Wang,H., Ye,S., Guan,J., Tan,W., Cheng,S., Wei,G., Wu,W., Wu,F. and Zhou,Y. (2012) Up-regulation of microRNA-126 may contribute to pathogenesis of ulcerative colitis via regulating NF-kappaB inhibitor IkappaBalpha. *PLoS One*, **7**, e52782.
79. Jiang,L., Lin,C., Song,L., Wu,J., Chen,B., Ying,Z., Fang,L., Yan,X., He,M., Li,J. *et al.* (2012) MicroRNA-30e* promotes human glioma cell invasiveness in an orthotopic xenotransplantation model by disrupting the NF-kappaB/IkappaBalpha negative feedback loop. *J. Clin. Invest.*, **122**, 33–47.
80. Huang,F., Tang,J., Zhuang,X., Zhuang,Y., Cheng,W., Chen,W., Yao,H. and Zhang,S. (2014) MiR-196a promotes pancreatic cancer progression by targeting nuclear factor kappa-B-inhibitor alpha. *PLoS One*, **9**, e87897.
81. Moody,R., Zhu,Y., Huang,Y., Cui,X., Jones,T., Bedolla,R., Lei,X., Bai,Z. and Gao,S.J. (2013) KSHV microRNAs mediate cellular transformation and tumorigenesis by redundantly targeting cell growth and survival pathways. *PLoS Pathog.*, **9**, e1003857.
82. Ye,S.B., Li,Z.L., Luo,D.H., Huang,B.J., Chen,Y.S., Zhang,X.S., Cui,J., Zeng,Y.X. and Li,J. (2014) Tumor-derived exosomes promote tumor progression and T-cell dysfunction through the regulation of enriched exosomal microRNAs in human nasopharyngeal carcinoma. *Oncotarget*, **5**, 5439–5452.
83. Zha,R., Guo,W., Zhang,Z., Qiu,Z., Wang,Q., Ding,J., Huang,S., Chen,T., Gu,J., Yao,M. *et al.* (2014) Genome-wide screening identified that miR-134 acts as a metastasis suppressor by targeting integrin beta1 in hepatocellular carcinoma. *PLoS One*, **9**, e87665.